Table 1
Control and SMA cases examined.

Control					SMA						
Case	Age/sex	Diagnosis	Cause of death	Postmortem time (h)	Case	Age/sex	Cause of death	Postmortem time (h)	Deletion patterns		SMA phenotype
									SMN	NAIP	
C1	17 w GA/M	FCMD	AA	3	S1	14 w GA/UK	AA	UK	E7, E8	E5, E6	UK
C2	18 w GA/M	FCMD	AA	<72	S2	20 w GA/UK	AA	UK	E7	Normal	UK
C3	21 w GA/F	Hydrops fetalis	SB	17.5							
C4	26 w GA/M	Cardiovascular anomaly	SB	10.5							
C5	31 w GA/F	Torsion of umbilical cord	SB	3							
C6	38 w GA/F	Polycystic kidney	SB	4							
C7	0 y 4 m/F	Cardiovascular anomaly	RF	2.5	S3	0 y 4 m/M	RF	2	E7, E8	Normal	Type 1
C8	0 y 6 m/M	Myotubular myopathy	AP, RF, HF	11.5	S4	0 y 5 m/F	RF	1	E7, E8	E5, E6	Type 1
C9	0 y 11 m/M	Cardiovascular anomaly	HF	2	S5	0 y 11 m/F	RF	1	E7, E8	Normal	Type 1
						0 y 11 m/F	RF	8	E7	Normal	Type 1
C10	5 y/M	Neuroblastoma	Metastasis	15.5	S7	5 y 6 m/M	RF	1	NE*	NE*	Type 1
C11	13 y/F	Cardiovascular anomaly	RF	8	S8	12 y 3 m/F	CA, Necrotic pancreatitis	3	E7, E8	Normal	Type 1
C12	17 y/M	FCMD	AP, RF, HF	8	S9	17 y/M	CA	3.5	E7, E8	Normal	Type 2
C13	18 y/F	Cardiovascular anomaly	HF	12							

Abbreviations: AA, artificial abortion; AP, acute pneumonia; CA, cardiac arrest; E, exon; F, female; FCMD, Fukuyama type congenital muscular dystrophy; GA, gestational age; HF, heart failure; M, male; NAIP, neuronal apoptosis inhibitor protein; NE, not examined; RF, respiratory failure; SB, stillbirth; UK, unknown.
* Elder brother of Case S5.

Louis, MO, USA) for 30 min at room temperature, quenched with 3% hydrogen peroxide for 20 min at room temperature, rinsed in Tris-buffered saline, pH 7.5 (TBS), and subsequently incubated with a reaction solution composed of 6 mU/μL TdT (GIBCO-BRL, Eggenstein, Germany) and 100 μM digoxigenin-11-conjugated dUTP (Roche Diagnostics, Mannheim, Germany) at final concentrations in distilled water-diluted TdT buffer under a humidified atmosphere for 60 min at 37 °C. The reaction was terminated by immersion in TBS for 30 min at 37 °C. After rinsing in TBS, sections were incubated for 30 min at room temperature with horseradish peroxidase (HRP)-labeled anti-digoxigenin antibody (Cat. No. 11593700; diluted 1:50; Roche). Immunoreaction products on sections were developed with DAB, and were counterstained with hematoxylin. Elimination of TdT in the reaction solution served as a negative control. Signals obtained by the TUNEL method were observed with a light microscope, and verified by comparison with H&E-stained consecutive sections.

3. Results

3.1. Histopathological observations

In the control cases, LMNs in the anterior horns demonstrated normal histopathological features in the fetal and postnatal periods. At 17, 18 and 21 weeks (w) of gestational age (GA), the LMNs showed physiological fetal immature profiles characterized by fine Nissl bodies restricted to the periphery of round somata with a few cell processes (Fig. 1a and c). At 31 and 38 w GA, the LMNs showed physiological fetal mature profiles characterized by fine Nissl bodies diffusely distributed in the cytoplasm of polygonal somata with the well-developed cell processes (Fig. 1d). At 0–18 y, the LMNs showed physiological postnatal mature profiles characterized by coarse Nissl bodies diffusely distributed in the cytoplasm of polygonal somata larger than those in the fetal period with preserved cell processes (Fig. 1f, h and j). The control spinal cords displayed no significant reactive gliosis. In the teenagers, a subset of the LMNs contained lipofuscin pigments (Fig. 1j). Both the anterior and posterior roots showed no significant morphological alteration (data not shown).

In the SMA cases, LMNs in the anterior horns demonstrated the characteristic histopathological features of SMA in the fetal and postnatal periods. In the fetal cases at 14 and 20 w GA, the LMNs showed pathological immature profiles characterized by fine Nissl bodies restricted to the periphery of round somata, smaller than those in the age-matched controls, as well as a few cell processes (Fig. 1b and e). In the postnatal cases at 0–17 y, the SMA spinal cords showed somatic reduction in size of the LMNs and appearance of ballooned

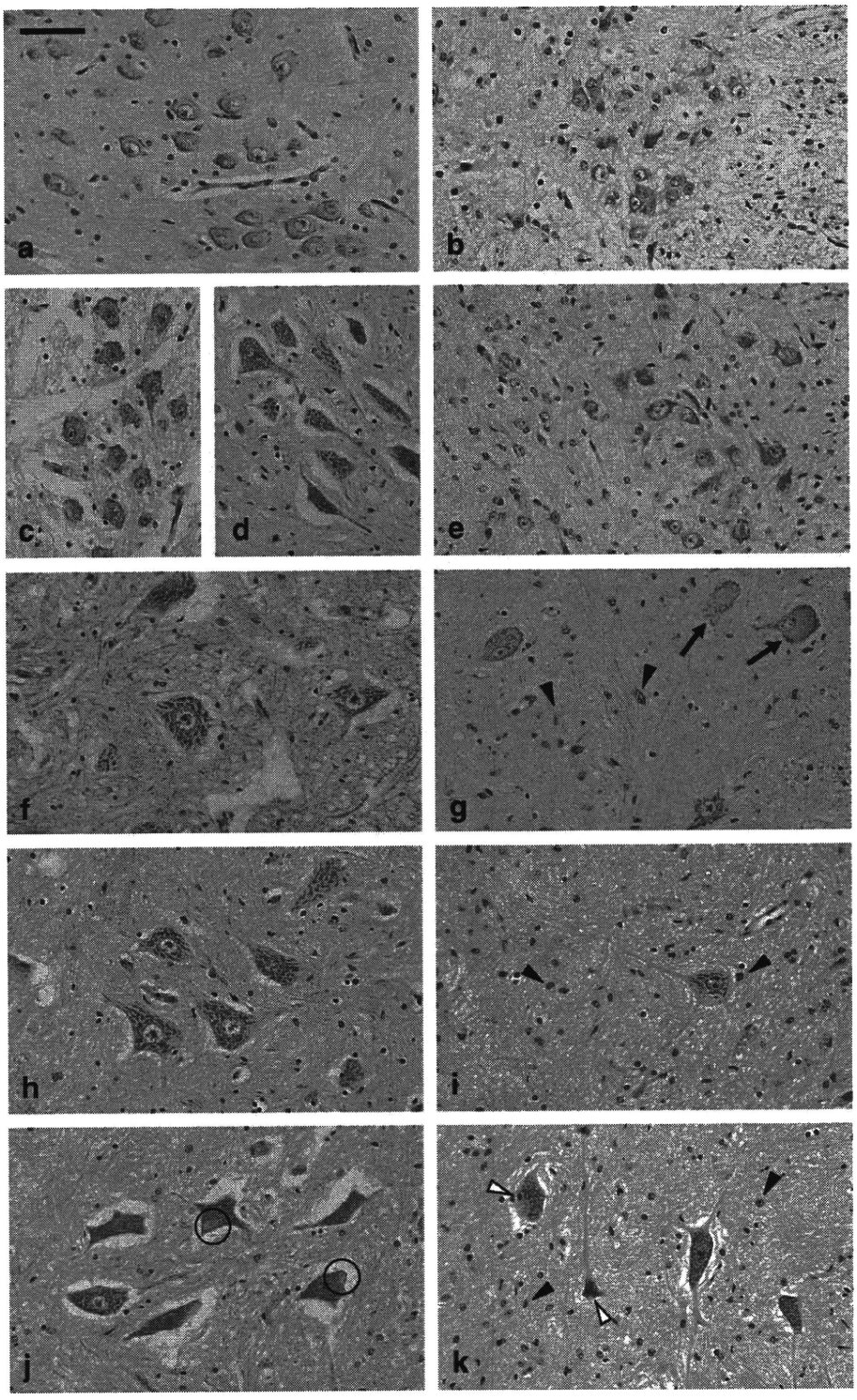

Fig. 1. Histopathological observations of motor neurons in hematoxylin–eosin-stained spinal cord anterior horn sections from the examined cases: 18 w (a), 21 w (c) and 31 w (d) GA control fetuses; 0 y 4 m (f); 0 y 11 m (h) and 18 y (j) control subjects; 14 w (b) and 20 w (e) GA SMA fetuses; 0 y 4 m (g), 0 y 11 m (i) and 17 y (k) SMA patients. Arrows and open circles indicate ballooned neurons and lipofuscin pigments, respectively. Blank and solid arrowheads indicate pyknotic nuclei of lower motor neurons and reactive astrocytes, respectively. Scale bar = 100 μm (a–k). *Abbreviations:* GA, gestational age; m, months old; SMA, spinal muscular atrophy; w, weeks; y, years old.

neurons (BNs), the latter evidenced by fragmentated or disappeared Nissl bodies in the cytoplasm of round somata with central or eccentric cell nucleus and reduced cell processes (Fig. 1g, i and k). BNs were smaller than typical chromatolytic neurons that have been shown to appear during axonal reaction in Wallerian

degeneration. Both the size and number of LMNs were evidently reduced in the SMA cases as compared to the age-matched controls, and the remaining LMNs including BNs diminished along with age. The population of survived LMNs was relatively preserved in the SMA type 2 Case S9, who lived to 17 y, as compared to the SMA type 1 Cases S3–S8. The severity of SMA symptoms correlated with the degree of a reduction in the number of LMNs. In the SMA teenagers, the anterior horns displayed both pyknotic cell nuclei (Fig. 1k) and lipofuscin pigments (data not shown) in a subset of the remaining LMNs as well as reactive astrocytosis. Additionally, glial bundles in the anterior roots of the SMA cases were found only in postnatal period, and those in the posterior roots were evident after 5 y, while those in SMA type 2 showed even milder change in the anterior roots and little change in the posterior roots (data not shown).

3.2. Immunohistochemical observations

No immunoreaction product deposit was visible on negative reaction control sections (data not shown) for the substances as mentioned below.

p-NFP immunoreactivity was mainly localized in axons in the gray and white matters of the postnatal control and SMA spinal cords (Fig. 2c, e and g). The immunoreactivity was undetectable in the cytoplasm of LMNs and glial cells in the fetal and postnatal control cases (Fig. 2g), while it was detectable only in the cytoplasm of BNs (Fig. 2e) but undetectable other neurons and glial cells in the fetal and postnatal SMA cases (Fig. 2a and c).

Ubiquitin immunoreactivity was weak but detectable only in the cell nucleus but undetectable in the cytoplasm of the LMNs in both the control and SMA spinal cords (Fig. 2b, d and h). Nuclear staining for ubiquitin was considered as a normal subcellular localizaton. BNs were only very weakly stained or not at all (Fig. 2f). Glial cells were negatively stained.

Bcl-2 immunoreactivity was prominent in the cytoplasm of the LMNs in the control and SMA groups in the early fetal period before 20 w GA (Fig. 3a and c), reduced around 20 w GA (Fig. 3b and d), and undetectable including BNs in the postnatal period (data not shown). There was no significant difference in staining in the LMNs between the SMA cases and the age-matched controls. Glial cells were negatively stained.

Bax immunoreactivity was prominent in the cytoplasm of the LMNs in the fetal control and SMA cases around 20 w GA (Fig. 3e and g). By contrast, it was undetectable in LMNs including BNs in the postnatal control and SMA cases (Fig. 3f and h). There was no significant difference in staining in the LMNs between the SMA cases and the age-matched controls. Glial cells were negatively stained.

Activated caspase-3 immunoreactivity was prominent in the cytoplasm of the LMNs in the fetal control and SMA cases around 20 w GA (Fig. 3i and k), with no significant difference in staining between the control and SMA groups. On the other side, the immunoreactivity was undetectable in the LMNs including BNs in the postnatal control and SMA cases (Fig. 3j and l). Most of the glial cells were negatively stained.

SMN immunoreactivity was localized in the cytoplasm of the LMNs in the control and SMA groups in the fetal and postnatal period (Fig. 4). The immunoreactivity was prominent in the fetal period (Fig. 4a and b) and within 5 years after birth (Fig. 4c–i), then reduced along with age, and at last disappeared in higher teenagers, with nonspecific deposits on lipofuscin pigments in the LMNs (Fig. 4j and k). The cytoplasm of BNs was also positive for SMN (Fig. 4g). There was no difference in staining pattern for SMN between the control and SMA groups. Most of the glial cells were negatively stained.

3.3. Observations on TUNEL-stained sections

Negative reaction control sections did not show any marked staining (data not shown). TUNEL-positive signals were undetectable in the cell nucleus and cytoplasm of LMNs of the fetal and postnatal control and SMA cases (Fig. 3m–p). By contrast, the signals were detectable in the nucleus of numerous glial cells and apoptotic bodies were rarely detectable in only a few glial cells from 21 and 26 w GA control fetuses, a 4-month-old control infant, and a 14 w GA SMA fetus (Fig. 3o).

4. Discussion

During development of the central and peripheral nervous system, half of the neuron population regresses and disappears [18]. The number of LMNs throughout the human spinal cord reduces from 11 to 25 w GA, but not thereafter [19]; this type of physiological cell death of LMNs overlaps with the initiation of functional muscular contact. In the present study, we tested the hypothesis that apoptosis may participate in the pathomechanism of SMA. Previous studies have suggested implications for the proapoptotic transcription factor p53 in SMA-associated LMN death [20]. p53 upregulates expression of the proapoptotic gene product Bax and downregulates expression of the antiaoptotic gene product Bcl-2 in the neurons [21], and is a pivotal molecule regulating the death of neurons during development and mediates a Bax-dependent caspase-3 activation in neuron [22]. Furthermore, Bax upregulation is involved in motor neuron death during physiological developmental processes [23]. Thus, our finding that the immunoreactivities for Bax and activated

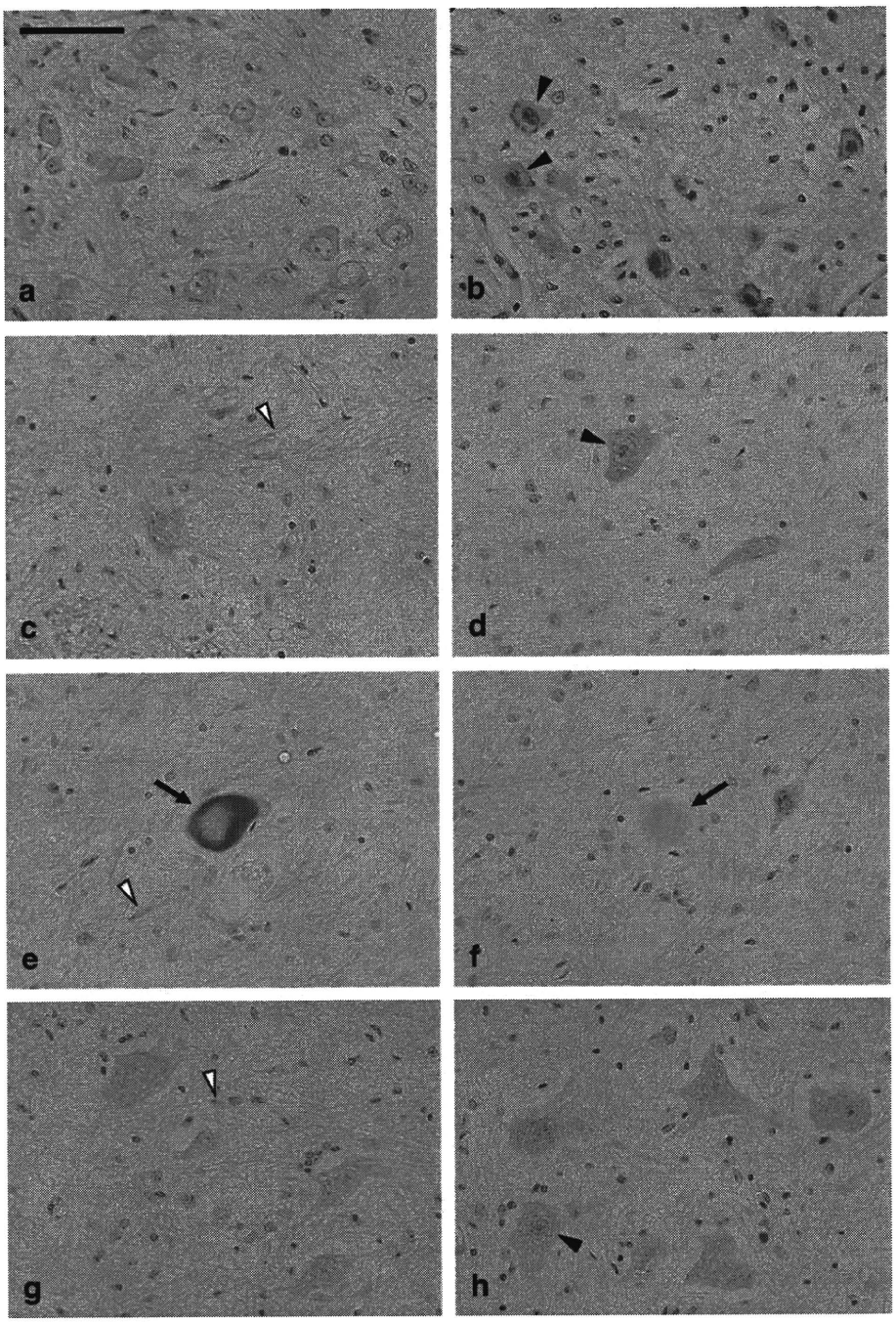

Fig. 2. Immunohistochemical staining for phosphorylated neurofilament protein (a, c, e and g) and ubiquitin (b, d, f and h) in motor neurons in spinal cord anterior horn sections from the examined cases: a 20 w GA SMA fetus (a and b); a 0 y 4 m SMA patient (c–f); and a 0 y 4 m control subject (g and h). Panels (e) and (f) indicate the same region on consecutive sections. Arrows and blank and solid arrowheads indicate ballooned neurons, axons and cell nuclei, respectively. Scale bar = 100 μm (a–h). *Abbreviations:* GA, gestational age; m, months old; SMA, spinal muscular atrophy; w, weeks; y, years old.

caspase-3 were detectable in the cytoplasm of a subset of the LMNs in both the control and SMA cases in the fetal period but not those in the postnatal period could indicate that p53-induced, Bax-mediated, caspase-3 activation occurs in these cells in relation to the normal developmental processes. The lack of TUNEL-positive signals in LMNs in the fetal and postnatal control and SMA spinal cords seemingly suggests a failure in caspase-mediated apoptosis in these cells. However, it is controversial whether TUNEL-positive signals are detectable or undetectable in SMA LMNs [16,24,25]. Moreover, given that apoptosis execution completes within some minutes after starting, followed by prompt scavenging of apoptotic cells by macrophages [26], it is

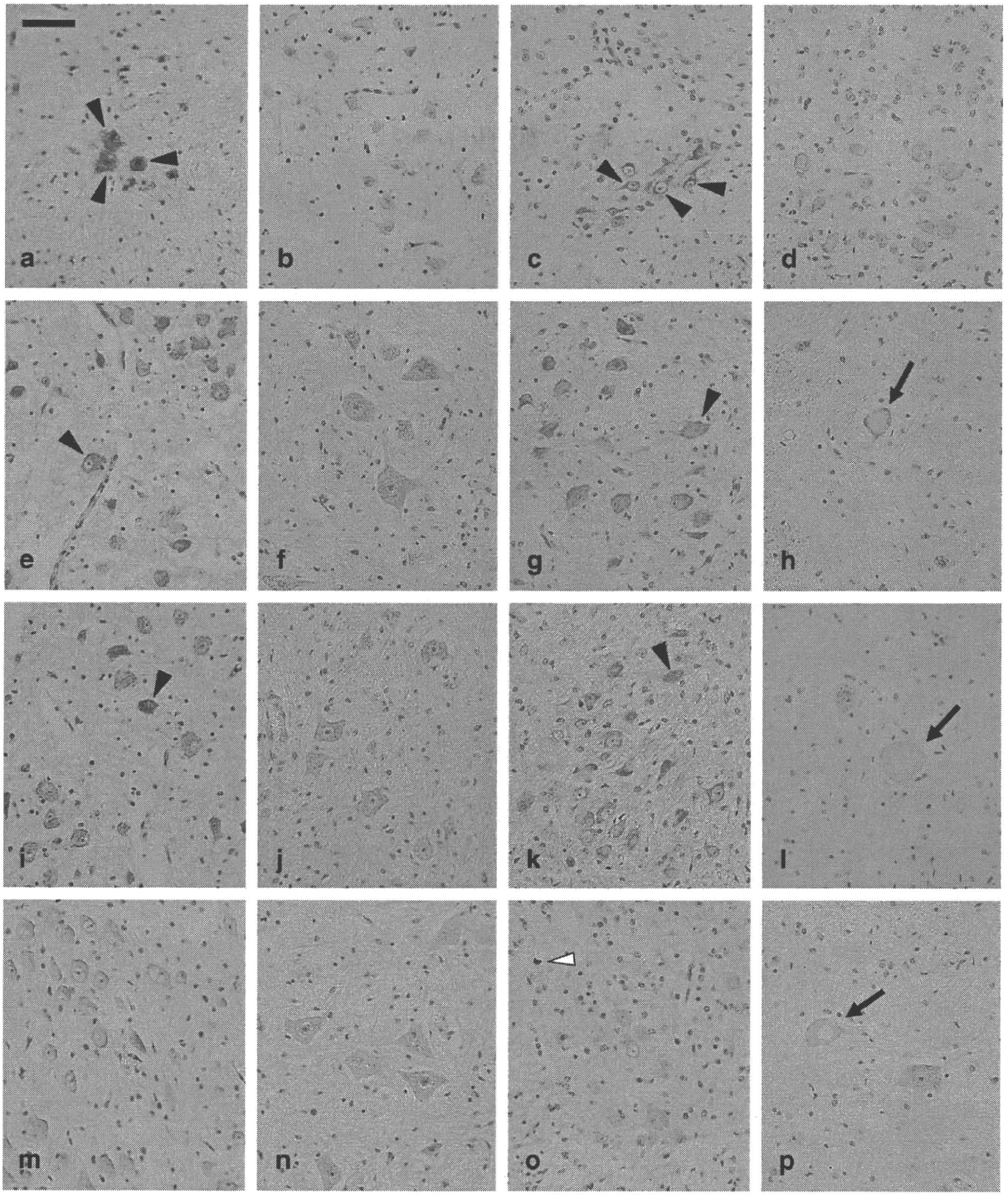

Fig. 3. Immunohistochemical staining for Bcl-2 (a–d), Bax (e–h) and activated caspase-3 (i–l) and terminal deoxynucleotidyl transferase-mediated dUTP nick end labeling (TUNEL) assay (m–p) in motor neurons in spinal cord anterior horn sections from the examined cases: 17 w (a), 18 w (m) and 21 w (b, e and i) GA control fetuses; a 0 y 4 m control subject (f, j and n); 20 w (d, g and k) and 14 w (c and o) GA SMA fetuses; and a 0 y 4 m SMA patient (h, l and p). Arrows and solid and blank arrowheads indicate ballooned neurons, immunoreactive cells and an astrocyte, respectively. Scale bar = 100 μm (a–p). *Abbreviations:* GA, gestational age; m, months old; SMA, spinal muscular atrophy; w, weeks; y, years old.

likely to be hard to detect morphological evidence for DNA fragmentation as a final event of apoptosis execution in originally hypocellular LMNs as compared to much more hypercellular neuroblasts or cancer cells on paraffin-embedded sections, using the TUNEL technique. On the other hand, we found the increased Bcl-2 levels in both the fetal control and SMA cases, suggesting that this protein interferes with Bax-dependent

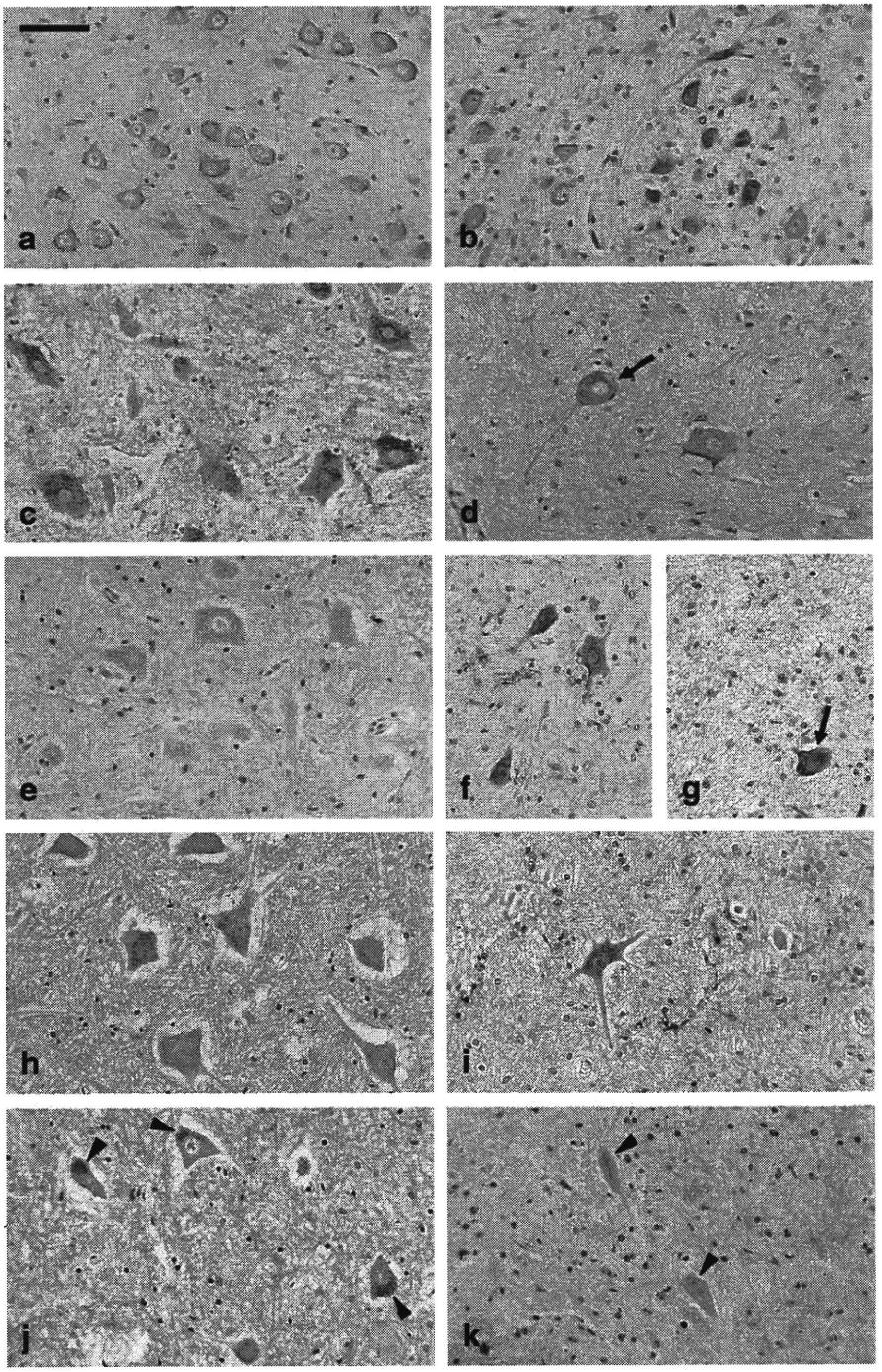

Fig. 4. Immunohistochemical staining for survival motor neuron protein in motor neurons in spinal cord anterior horn sections from the examined cases: a 18 w GA control fetus (a); 0 y 4 m (c), 0 y 11 m (e), 5 y (h) and 18 y (j) control subjects; a 20 w GA SMA fetus (b); and 0 y 4 m (d), 0 y 11 m (f and g), 5 y (i) and 17 y (k) SMA patients. Arrows and arrowheads indicate ballooned neurons and lipofuscin pigments, respectively. Scale bar = 100 μm (a–k). *Abbreviations:* GA, gestational age; m, months old; SMA, spinal muscular atrophy; w, weeks; y, years old.

apoptosis in the fetal period, as similar processes occur in developmental LMN death [27]. Although a previous study showed downregulation of Bcl-2 in SMA fetuses [28], it is difficult to disclose a difference in Bcl-2 expression levels between the control and SMA groups by morphological approaches as indicated here. If pathological analyses are performed in SMA fetus after 20 w GA onward, maybe we will gain the evidences of accelerated apoptosis in SMA during advanced stage of pregnancy.

Several studies have indicated that the pathognomonic, histopathological hallmarks of SMA in the postnatal cases are loss of motor neurons, appearance of BNs and reactive astrocytosis in the anterior horns as well as

the formation of glial bundles in the anterior roots [1,29,30]. In the present study, as another issue, we focused on histopathological changes in the spinal cord of SMA fetuses. Small-sized profiles of LMNs in the fetal and postnatal SMA cases and severe motor neuron loss after birth in our study suggests that LMN insult had begun in the fetal period. The fact that fetal SMA cases showed the pathological immature profiles is consistent with a previous report showing the immaturity of LMNs in SMA [31]. In the report, LMNs in fetal and infantile SMA cases displayed a smaller size than age-matched controls as well as less developed Nissl bodies restricted to the periphery of the cytoplasm, suggesting the involvement of a failure in the formation of adequate neuromuscular contact in neuronal cell death. However, this is controversial because another report on motor neuronal death during development has indicated that both the morphology and the mean nuclear diameters of LMNs in SMA cases were similar to those in control cases [15]. In the spinal cord of infantile SMA cases, we found BNs, which showed fragmentated or disappeared Nissl bodies in round somata with the eccentric or central cell nucleus and reduced cell processes. These observations could indicate the similarity of BNs to chromatolytic neurons, which have been shown to appear as "axonal reaction" in Wallerian degeneration following axotomy [32]. However, the finding that the size of BNs in SMA was smaller than that of typical chromatolytic neurons points to the possibility that other concomitant mechanisms such as impairment of neuronal maturation and neuromuscular contact may be involved in this disease. In this respect, it is of interest that a simultaneous upregulation of both Bcl-2 and Bax results from axonal insult, as shown in sciatic nerve injury [33]. In our study, like chromatolytic neurons, all of the BNs were filled with p-NFP as described previously by different investigators [25,30,34–36]. On the other hand, it is controversial whether BNs may be ubiquitinated [30,34,36,37]. Since a disruption of the ubiquitin–proteasome system against intracellular protein accumulation is involved in cell survival or death [38], our finding that BNs contained p-NFP accumulations and lacked ubiquitin (Fig. 2e and f) suggests a consequence of stagnant axonal transport without subsequent activation of the system against the accumulating p-NFP.

We also evaluated implications for SMN in the pathomechsnim of SMA, using an immunohistochemical approach. SMN has been shown to be localized in the cytoplasm of the soma, nuclear structures called gems, axons, dendrites and neuromuscular junctions of the LMNs [17,39–42]. In this study, SMN immunoreactivity in the cytoplasm of the soma and cell processes of the LMNs was prominent in the control and SMA cases in the fetal period and within 5 years after birth but in contrast less intense in the teenagers. This is in keeping with previous evidence for the age-dependent reduction in SMN expression levels [7,8]. Our finding of the presence of SMN immunoreactivity in the LMNs, including BNs, in both the SMA and age-matched control groups suggest that the SMN-specific antibody 2B1 used in our study recognizes both wildtype and mutant proteins. This is supported by evidence that the epitope of the antibody 2B1 is the amino terminus of SMN protein encoded by exon 1 [9], which is perceived in all SMA phenotypes and SMN gene mutations. SMN has been shown to play important roles in a post-transcriptional mechanism in the cell nucleus [17]. In addition, precedent investigations have provided evidence that SMN not only exerts antiapoptotic effects by itself [43,44] but also participates in antiapoptotic mechanism through the inhibitory interaction with p53 [20] and the synergistic interaction with Bcl-2 [45], although subsequent studies did not support the latter interaction [46,47]. Recent studies have suggested another function of SMN, which may be involved in nucleocytoplasmic, dendritic or axonal transport [40,41,46] and neurite outgrowth and neuromuscular maturation during differentiation and development of the neurons [39].

Taken together, we here demonstrated several findings obtained from histopathological, immunohistochemical and TUNEL analyses on the spinal cord of control and SMA cases in the fetal and postnatal periods. In spite of the detection of Bax and activated caspase-3 in both the control and SMA cases in the fetal period, the present results did not provide convincing evidence for apoptosis closely relevant to SMA. Both the pathological immature profiles and the reduced size of LMNs in the early fetal SMA cases as compared to the age-matched controls suggest a critical role for impaired neuronal development. As indicated in Fig. 5, we postulate the hypothesis that SMA may be

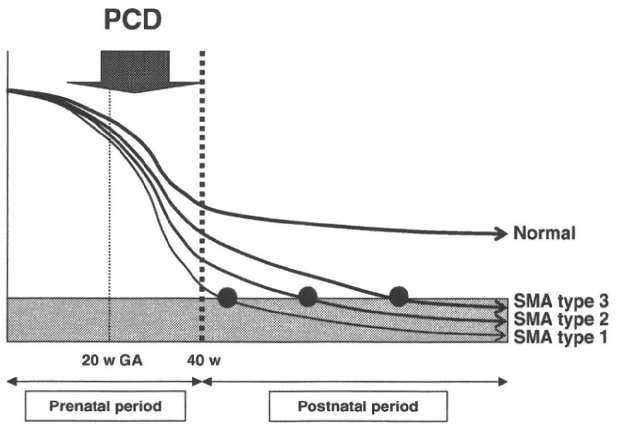

Fig. 5. A schematic diagram showing changes in the number of lower motor neurons (LMN) in the spinal cord anterior horns of control and spinal muscular atrophy (SMA) and comparison of the disease severity among SMA types 1, 2 and 3. Large and small arrows indicate prenatal programmed cell death (PCD) and postnatal retrograde degeneration of LMN, respectively. Gray zones and solid dots indicate a critical level of clinical manifestations and age at onset, respectively.

a fetal developmental maturation error as well as a postnatal retrograde dying-back degeneration of LMNs. Under physiological conditions, immature LMNs are eliminated by PCD in the fetal period to some extent, and then the remaining mature LMNs survive in the postnatal period. In the case of SMA, since the down-regulation of SMN impairs neuromuscular maturation and neurite outgrowth [39], it is likely that elimination of immature LMNs is accelerated during advanced stage of pregnancy when we cannot find true fact without stillbirth, while loss of the residual small-sized LMNs continues in the postnatal period. Among the SMA phenotypes, the clinical features are the most severe in type 1 and milder in types 2 and 3, because the residual motor function depends on the number of the remaining LMNs. When the number of LMNs decreases to a critical level (Fig. 5), motor symptoms may be apparent. Our hypothesis does not contradict the involvement of PCD in SMA, and it might even explain differences in age at onset between the clinical phenotypes. Postnatal retrograde dying-back degeneration is supported by studies on a mutant SMN transgenic mouse model of SMA, which demonstrate the neurofilamentous accumulation at motor endplate, more severely affected axons than cell bodies of LMNs, the lack of axonal sprouting of LMNs [48], and muscular atrophy preceding LMNs loss [49]. Further investigations oriented to these issues may contribute to better understanding of SMA. It is predicted that trials of intrauterine therapy would be beneficial for this disease.

Acknowledgements

We thank Dr. Gideon Dreyfuss for generously providing a monoclonal anti-SMN antibody 2B1, and Mr. M. Karita for technical assistance. This study was supported, in part, by a grant from the Morinaga Foundation for Health & Nutrition.

References

[1] Osawa M, Shishikura K. Werdnig-Hoffmann disease and variants. In: Vinken PJ, Bruyn GW, Klawans HL, Vianney de Jong JM, editors, Handbook of clinical neurology, vol. 15, Diseases of the Motor System. Amsterdam. New York: Elsevier; 1991. p. 51–80.

[2] Munsat TL, Davies KE. Meeting report: International SMA consortium meeting, Bonn, 1992. Neuromuscul Disord 1992;2:423–8.

[3] Lefebvre S, Burglen L, Reboullet S, Clermont O, Burlet P, Viollet L, et al. Identification and characterization of a spinal muscular atrophy-determining gene. Cell 1995;80:155–65.

[4] Monani UR, Lorson CL, Parsons DW, Prior TW, Androphy EJ, Burghes AH, et al. A single nucleotide difference that alters splicing patterns distinguishes the SMA gene SMN1 from the copy gene SMN2. Hum Mol Genet 1999;8:1177–83.

[5] Roy N, Mahadevan MS, McLean M, Shutler G, Yaraghi Z, Farahani R, et al. The gene for neuronal apoptosis inhibitory protein is partially deleted in individuals with spinal muscular atrophy. Cell 1995;80:167–78.

[6] Burglen L, Seroz T, Miniou P, Lefebvre S, Burlet P, Munnich A, et al. The gene encoding p44, a subunit of the transcription factor TFIIH, is involved in large-scale deletions associated with Werdnig-Hoffmann disease. Am J Hum Genet 1997;60:72–9.

[7] Burlet P, Huber C, Bertrandy S, Ludosky MA, Zwaenepoel I, Clermont O, et al. The distribution of SMN protein complex in human fetal tissues and its alteration in spinal muscular atrophy. Hum Mol Genet 1998;7:1927–33.

[8] La Bella V, Cisterni C, Salaun D, Pettmann B. Survival motor neuron (SMN) protein in rat is expressed as different molecular forms and is developmentally regulated. Eur J Neurosci 1998;10:2913–23.

[9] Lefebvre S, Burlet P, Liu Q, Bertrandy S, Clermont O, Munnich A, et al. Correlation between severity and SMN protein level in spinal muscular atrophy. Nat Genet 1997;16:265–9.

[10] Coovert DD, Le TT, McAndrew PE, Strasswimmer J, Crawford TO, Mendell JR, et al. The survival motor neuron protein in spinal muscular atrophy. Hum Mol Genet 1997;6:1205–14.

[11] Campbell L, Potter A, Ignatius J, Dubowitz V, Davies K. Genomic variation and gene conversion in spinal muscular atrophy: implications for disease process and clinical phenotype. Am J Hum Genet 1997;61:40–50.

[12] Araki S, Hayashi M, Tamagawa K, Saito M, Kato S, Komori T, et al. Neuropathological analysis in spinal muscular atrophy type II. Acta Neuropathol (Berl) 2003;106:441–8.

[13] Kuru S, Sakai M, Konagaya M, Yoshida M, Hashizume Y, Saito K. An autopsy case of spinal muscular atrophy type III (Kugelberg-Welander disease). Neuropathology 2009;29:63–7.

[14] Fidzianska A, Rafalowska J. Motoneuron death in normal and spinal muscular atrophy-affected human fetuses. Acta Neuropathol (Berl) 2002;104:363–8.

[15] Soler-Botija C, Ferrer I, Gich I, Baiget M, Tizzano EF. Neuronal death is enhanced and begins during foetal development in type I spinal muscular atrophy spinal cord. Brain 2002;125:1624–34.

[16] Simic G, Seso-Simic D, Lucassen PJ, Islam A, Krsnik Z, Cviko A, et al. Ultrastructural analysis and TUNEL demonstrate motor neuron apoptosis in Werdnig-Hoffmann disease. J Neuropathol Exp Neurol 2000;59:398–407.

[17] Liu Q, Dreyfuss G. A novel nuclear structure containing the survival of motor neurons protein. EMBO J 1996;15:3555–65.

[18] Oppenheim RW. Cell death during development of the nervous system. Annu Rev Neurosci 1991;14:453–501.

[19] Forger NG, Breedlove SM. Motoneuronal death during human fetal development. J Comp Neurol 1987;264:118–22.

[20] Young PJ, Day PM, Zhou J, Androphy EJ, Morris GE, Lorson CL. A direct interaction between the survival motor neuron protein and p53 and its relationship to spinal muscular atrophy. J Biol Chem 2002;277:2852–9.

[21] Lu J, Moochhala S, Kaur C, Ling EA. Changes in apoptosis-related protein (p53, Bax, Bcl-2 and Fos) expression with DNA fragmentation in the central nervous system in rats after closed head injury. Neurosci Lett 2000;290:89–92.

[22] Cregan SP, MacLaurin JG, Craig CG, Robertson GS, Nicholson DW, Park DS, et al. Bax-dependent caspase-3 activation is a key determinant in p53-induced apoptosis in neurons. J Neurosci 1999;19:7860–9.

[23] Sato N, Sakuma C, Sato Y, Gould TW, Oppenheim RW, Yaginuma H. Distinct susceptibility of developing neurons to death following Bax overexpression in the chicken embryo. Cell Death Differ 2006;13:435–45.

[24] Hayashi M, Arai N, Murakami T, Yoshio M, Oda M, Matsuyama H. A study of cell death in Werdnig Hoffmann disease brain. Neurosci Lett 1998;243:117–20.

[25] Pumarola M, Anor S, Majo N, Borras D, Ferrer I. Spinal muscular atrophy in Holstein-Friesian calves. Acta Neuropathol (Berl) 1997;93:178–83.
[26] Kuan C-Y, Roth KA, Flavell RA, Rakic P. Mechanisms of programmed cell death in the developmental brain. Trends Neurosci 2000;23:291–7.
[27] Yuan J, Lipinski M, Degterev A. Diversity in the mechanisms of neuronal cell death. Neuron 2003;40:401–13.
[28] Soler-Botija C, Ferrer I, Alvarez JL, Baiget M, Tizzano EF. Downregulation of Bcl-2 proteins in type I spinal muscular atrophy motor neurons during fetal development. J Neuropathol Exp Neurol 2003;62:420–6.
[29] Ikemoto A, Hirano A, Matsumoto S, Akiguchi I, Kimura J. Synaptophysin expression in the anterior horn of Werdnig-Hoffmann disease. J Neurol Sci 1996;136:94–100.
[30] Murayama S, Bouldin TW, Suzuki K. Immunocytochemical and ultrastructural studies of Werdnig-Hoffmann disease. Acta Neuropathol (Berl) 1991;81:408–17.
[31] Fidzianska A, Rafalowska J, Glinka Z. Ultrastructural study of motoneurons in Werdnig-Hoffmann disease. Clin Neuropathol 1984;3:260–5.
[32] Price DL, Porter KR. The response of ventral horn neurons to axonal transection. J Cell Biol 1972;53:24–37.
[33] Gillardon F, Klimaschewski L, Wickert H, Krajewski S, Reed JC, Zimmermann M. Expression pattern of candidate cell death effector proteins Bax, Bcl-2, Bcl-X, and c-Jun in sensory and motor neurons following sciatic nerve transaction in the rat. Brain Res 1996;739:244–50.
[34] Urbanits S, Budka H. Spinal pathology in spinal muscular atrophy in comparison with amyotrophic lateral sclerosis (in German). Wien Med Wochenschr 1996;146:199–200.
[35] Lippa CF, Smith TW. Chromatolytic neurons in Werdnig-Hoffmann disease contain phosphorylated neurofilaments. Acta Neuropathol (Berl) 1988;77:91–4.
[36] Kato S, Hirano A. Ubiquitin and phosphorylated neurofilament epitopes in ballooned neurons of the extraocular muscle nuclei in a case of Werdnig-Hoffmann disease. Acta Neuropathol (Berl) 1990;80:334–7.
[37] Hiraga T, Leipold HW, Cash WC, Troyer DL. Reduced numbers and intense anti-ubiquitin immunostaining of bovine motor neurons affected with spinal muscular atrophy. J Neurol Sci 1993;118:43–7.
[38] Rogers N, Paine S, Bedford L, Layfield R. The ubiquitin–proteasome system: contributions to cell death or survival in neurodegeneration. Neuropathol Appl Neurobiol 2010;36: 113–24.
[39] Fan L, Simard LR. Survival motor neuron (SMN) protein: role in neurite outgrowth and neuromuscular maturation during neuronal differentiation and development. Hum Mol Genet 2002;11:1605–14.
[40] Pagliardini S, Giavazzi A, Setola V, Lizier C, Di Luca M, DeBiasi S, et al. Subcellular localization and axonal transport of the survival motor neuron (SMN) protein in the developing rat spinal cord. Hum Mol Genet 2000;9:47–56.
[41] Bechade C, Rostaing P, Cisterni C, Kalisch R, La Bella V, Pettmann B, et al. Subcellular distribution of survival motor neuron (SMN) protein: possible involvement in nucleocytoplasmic and dendritic transport. Eur J Neurosci 1999;11: 293–304.
[42] Broccolini A, Engel WK, Askanas V. Localization of survival motor neuron protein in human apoptotic-like and regenerating muscle fibers, and neuromuscular junctions. Neuroreport 1999;10:1637–41.
[43] Vyas S, Bechade C, Riveau B, Downward J, Triller A. Involvement of survival motor neuron (SMN) protein in cell death. Hum Mol Genet 2002;11:2751–64.
[44] Kerr DA, Nery JP, Traystman RJ, Chau BN, Hardwick JM. Survival motor neuron protein modulates neuron-specific apoptosis. Proc Natl Acad Sci USA 2000;97:13312–7.
[45] Iwahashi H, Eguchi Y, Yasuhara N, Hanafusa T, Matsuzawa Y, Tsujimoto Y. Synergistic anti-apoptotic activity between Bcl-2 and SMN implicated in spinal muscular atrophy. Nature 1997;390:413–7.
[46] La Bella V, Kallenbach S, Pettmann B. Expression and subcellular localization of two isoforms of the survival motor neuron protein in different cell types. J Neurosci Res 2000;62: 346–56.
[47] Coovert DD, Le TT, Morris GE, Man NT, Kralewski M, Sendtner M, et al. Does the survival motor neuron protein (SMN) interact with Bcl-2? J Med Genet 2000;37:536–9.
[48] Cifuentes-Diaz C, Nicole S, Velasco ME, Borra-Cebrian C, Panozzo C, Frugier T, et al. Neurofilament accumulation at the motor endplate and lack of axonal sprouting in a spinal muscular atrophy mouse model. Hum Mol Genet 2002;11:1439–47.
[49] Frugier T, Tiziano FD, Cifuentes-Diaz C, Miniou P, Roblot N, Dierich A, et al. Nuclear targeting defect of SMN lacking the C-terminus in a mouse model of spinal muscular atrophy. Hum Mol Genet 2000;9:849–58.

Journal of Cellular Physiology

Cells of Extraembryonic Mesodermal Origin Confer Human Dystrophin in the Mdx Model of Duchenne Muscular Dystrophy

YAYOI KAWAMICHI,[1,2,3] CHANG-HAO CUI,[1] MASASHI TOYODA,[1] HATSUNE MAKINO,[1] AKANE HORIE,[1] YORIKO TAKAHASHI,[1] KENJI MATSUMOTO,[4] HIROHISA SAITO,[4] HIROAKI OHTA,[2] KAYOKO SAITO,[3] AND AKIHIRO UMEZAWA[1]*

[1]*Department of Reproductive Biology, National Institute for Child Health and Development, Tokyo, Japan*

[2]*Department of Obstetrics and Gynecology, Tokyo Women's Medical University, Tokyo, Japan*

[3]*Institute of Medical Genetics, Tokyo Women's Medical University, Tokyo, Japan*

[4]*Department of Allergy and Immunology, National Institute for Child Health and Development, Tokyo, Japan*

Duchenne muscular dystrophy is an X-linked recessive genetic disease characterized by severe skeletal muscular degeneration. The placenta is considered to be a promising candidate cell source for cellular therapeutics because it contains a large number of cells and heterogenous cell populations with myogenic potentials. We analyzed the myogenic potential of cells obtained from six parts of the placenta, that is, umbilical cord, amniotic epithelium, amniotic mesoderm, chorionic plate, villous chorion, and decidua basalis. In vitro cells derived from amniotic mesoderm, chorionic plate, and villous chorion efficiently transdifferentiate into myotubes. In addition, in vivo implantation of placenta-derived cells into dystrophic muscles of immunodeficient mdx mice restored sarcolemmal expression of human dystrophin. Differential contribution to myogenesis in this study may be attributed to placental portion-dependent default cell state. Molecular taxonomic characterization of placenta-derived maternal and fetal cells in vitro will help determine the feasibility of cell-based therapy.

J. Cell. Physiol. 223: 695–702, 2010.

The human placenta is a large discoid organ with a diameter of around 20 cm and a weight of approximately 500 g. It contains a large number of cells possessing a wide range of phenotypes and potentials (Cunningham and Williams, 2005; Sadler and Langman, 2006). The functions of the placenta are (a) exchange of metabolic and gaseous products between maternal and fetal bloodstreams and (b) production of hormones, such as progesterone, estradiol, estrogen, and human chorionic gonadotrophin. The placenta consists of the following two components: (a) a fetal portion, derived from the amnion, the chorionic plate (CP), the smooth chorion (chorion laeve (SC)), and the villous chorion (chorion frondosum (VC)) and (b) a maternal portion, derived from the decidua basalis (DB). The amnion, the inner layer, consists of a small amount of connective tissue (amniotic mesoderm (AM)) covered with a cuboidal epithelium (amniotic epithelium (AE)). The amniogenesis is rather complicated, the AM being extraembryonic whereas the AE is from the inner cell mass/embryoblast. The chorion, the outer layer of the amnion, is classified into VC, SC, and CP. The embryonic and abembryonic portions are called villous and SC, respectively. The VC is made of growing and expanding villi, while the CP and SC are made of degenerated villi. The DB, originating from the endometrium, is composed of glandular epithelial cells and stromal (mesenchymal) cells with decidual change. The umbilical cord (UC) that attaches a fetus to the placenta develops from the body stalk of the embryo and contains blood vessels and Wharton jelly, surrounded by the amnion. Each part of the placenta has recently been a candidate cell source for cell-based therapies because of the variety of cell types that become available (Fukuchi et al., 2004; Portmann-Lanz et al., 2006).

One currently untreatable disease which may benefit from cell-based therapy using placenta-derived cells is Duchenne muscular dystrophy (DMD). DMD is an X-linked recessive genetic disease characterized by severe skeletal muscle degeneration. It is caused by a deficiency in dystrophin that is associated with a large oligomeric complex of glycoproteins which provide linkage to the extracellular membrane (Ervasti and Campbell, 1991). The absence of dystrophin results in destabilization of the extracellular membrane–sarcolemma–cytoskeleton architecture, making muscle fibers susceptible to contraction-associated mechanical stress and degeneration. In the first phase of the disease, new muscle fibers are formed by satellite cells. After depletion of the satellite cell pool in

Yayoi Kawamichi, Chang-Hao Cui, and Masashi Toyoda contributed equally to this work.

Additional Supporting Information may be found in the online version of this article.

Contract grant sponsor: Ministry of Health, Labour and Welfare (Nervous and Mental Disorders);
Contract grant number: 18A-1, 19A-7 and 20B-13.
Contract grant sponsor: Japan Health Sciences Foundation;
Contract grant number: KHD1026.
Contract grant sponsor: Ministry of Health, Labour and Welfare (Child Health and Development);
Contract grant number: 21A-3.

*Correspondence to: Akihiro Umezawa, National Institute for Child Health and Development, 2-10-1, Okura, Setagaya, Tokyo 157-8535, Japan. E-mail: umezawa@1985.jukuin.keio.ac.jp

Received 25 August 2009; Accepted 22 December 2009

Published online in Wiley InterScience (www.interscience.wiley.com.), 16 February 2010.
DOI: 10.1002/jcp.22076

childhood, skeletal muscles degenerate progressively and irreversibly and are replaced by fibrotic tissue (Cossu and Mavilio, 2000). No effective therapeutic approaches for muscular dystrophy currently exist; thus, cell-based therapy, in addition to gene therapy (Harper et al., 2002), exon skipping therapy (Matsuo et al., 1991), and read-through therapy by aminoglycoside (Barton-Davis et al., 1999) remain promising treatment options.

Myoblasts represent the natural first choice in cellular therapeutics for skeletal muscle because of their intrinsic myogenic commitment (Grounds et al., 2002). However, myoblasts recovered from muscular biopsies are poorly expandable in vitro and rapidly undergo senescence (Cossu and Mavilio, 2000). Intramuscular allotransplantation of normal muscle precursor cells can induce expression of donor-derived dystrophin in skeletal muscles of patients with DMD (Skuk et al., 2006). However, it is difficult to perform transplantation of muscle precursor cells due to a limited number of donor cells. An alternative source of muscle progenitor cells is therefore desirable. Cells with a myogenic potential are present in many tissues, including bone marrow (Ferrari et al., 1998; Dezawa et al., 2005), UC blood (Gang et al., 2004), adipose tissue (Rodriguez et al., 2005; Di Rocco et al., 2006), and endometrium and menstrual blood (Cui et al., 2007), and all these cells readily form skeletal muscle in culture.

There has, as yet, been no systematic analysis of the distribution of placenta-derived stem cells which have myogenic differentiation potential. Therefore, we characterized each placenta-derived cell in vitro, via a taxonomic approach using global gene expression profiles, and investigated which part of the placenta is the most useful source of stem cells with a myogenic potential that might prove useful for possible future cell-based therapy of DMD.

Materials and Methods

Isolation of human placental tissues

Ethical approval for tissue collection was granted by the Institutional Review Board of the National Institute for Child Health and Development, Japan. Written informed consent was obtained before the sample collection. Human placental samples were collected from normal full-term pregnancies. All of the placentas were processed within 24 h of collection and washed extensively with phosphate-buffered saline (PBS). After peeling off the amnion, the placenta was separated into three parts, that is, CP, VC, and DB. To isolate cells from the UC, the middle part was used, after excluding the edge of the placenta and the tissue close to the fetal navel. The amnion and the SC were manually separated. Amniotic mesodermal cells were manually scraped from the AE. After each placental part was minced using scissors, minced AM was re-suspended in MSCGM (Cambrex Bio Science, Walkersville, MD). We did not calculate the cell numbers at the start of cultivation because the tissue was chopped up mechanically by hand. The placenta-derived cells were maintained at 37°C in a humidified atmosphere containing 5% CO_2 and allowed to attach for 48 h. Non-adherent cells were removed and the medium was changed twice a week. At 70–80% confluence, the cells were harvested with trypsin (0.25%) and 1 mM EDTA (0.02%) in PBS (1:1, v/v) and plated to new dishes. Primary culture cells were used, except for the differentiation analysis. Cells were processed from 45 placentas, and primary cultures from 10 placentas were used for this study.

Flow cytometric analysis

Flow cytometric analysis was performed as previously described (Terai et al., 2005). Briefly, cells were incubated with primary antibodies or isotype-matched control antibodies, followed by additional treatment with the immunofluorescent secondary antibodies. Cells were analyzed on an EPICS ALTRA analyzer (Beckman Coulter, Fullerton, CA). Antibodies against human CD13, CD14, CD29, CD34, CD44, CD45, CD55, CD59, CD73, CD90, CD105, CD166, HLA-ABC, and HLA-DR were purchased from Beckman Coulter, Immunotech (Marseille, France), Cytotech (Hellebaek, Denmark), and BD Biosciences Pharmingen (San Diego, CA).

In vitro myogenesis

In vitro myogenic analysis was performed as previously described (Cui et al., 2007). Briefly, placenta-derived cells were seeded onto 60-mm collagen I-coated cell culture dishes (BD Biocoat™) at a density of 1×10^4/ml in growth medium (Dulbecco's modified Eagle's medium (DMEM), supplemented with 20% fetal bovine serum (FBS)). Forty-eight hours after seeding onto collagen I-coated dishes, the cells were treated with 5 μm 5-azacytidine for 24 h. Cell cultures were then maintained in differentiation medium (DMEM, supplemented with 2% horse serum). The differentiation medium was changed twice a week until the experiment was terminated.

Reverse transcriptase-polymerase chain reaction analysis (RT-PCR) of placenta-derived cells

RT-PCR analysis was performed as previously described (Cui et al., 2007). Briefly, RT-PCR of MyoD, Myf5, myogenin, myosin heavy chain-IIx/d (MyHC-IIx/d), desmin, and dystrophin was performed with 2 μg of total RNA. The sequences of PCR primers that amplify human but not mouse genes are listed in Supplementary Table 1. PCR was performed for 30 cycles, with each cycle consisting of 94°C for 30 sec, 60°C or 65°C for 30 sec, and 72°C for 20 sec, with additional 10-min incubation at 72°C after completion of the last cycle.

Fusion assay in vitro

Placenta-derived cells (2,500/cm^2) were co-cultured with C2C12 myoblasts (2,500/cm^2) for 2 days in DMEM supplemented with 10% FBS, and then cultured for seven additional days in DMEM with 2% horse serum to promote myotube formation. C2C12 myoblast cells were supplied by RIKEN Cell Bank (The Institute of Physical and Chemical Research, Japan). The cultures were fixed in 4% paraformaldehyde (PFA) and stained with a mouse anti-human nuclei IgG1 monoclonal antibody (clone 235-1, Millipore, Billerica, MA) and a mouse anti-myosin heavy chain IgG2b monoclonal antibody (MF-20, Developmental Studies Hybridoma Bank, University of Iowa, IA). The cells were visualized with appropriate Alexa-fluor-conjugated goat anti-mouse IgG1 and IgG2b secondary antibodies (Molecular Probes, Eugene, OR). Total cell nuclei were stained with 4′, 6-diamidino-2-phenylindole (DAPI). To assess the ability of placenta-derived cells to fuse with C2C12 cells, we calculated the percentage of myotubes containing one or more human nuclei in the total myotube as a fusion index.

In vivo cell implantation

The cells (2×10^7) were suspended in PBS, in a total volume of 100 μl, and directly injected into the right tibialis anterior muscle of 6- to 8-week-old mdx/mdx scid/scid (mdx-scid) mice. The mice were euthanized 4 weeks after cell implantation, and the right tibialis anterior muscle was analyzed for human dystrophin by immunohistochemistry.

Immunohistochemical and immunocytochemical analysis

Immunohistochemical and immunocytochemical analyses were performed as previously described (Mori et al., 2005). Briefly, the sections were incubated with a mouse anti-human dystrophin IgG2a monoclonal antibody (NCL-DYS3, Novocastra, UK), and then incubated with horseradish peroxidase-conjugated rabbit anti-mouse immunoglobulin. Staining was developed using a solution containing diaminobenzidine and H_2O_2. Slides were

counterstained with hematoxylin. In the cases of fluorescence, frozen sections fixed with 4% PFA were used. The anti-human dystrophin monoclonal antibody, anti-human nuclei mouse monoclonal antibody, anti-α-sarcoglycan rabbit IgG polyclonal antibody (H-82, Santa Cruz Biotechnology, Santa Cruz, CA) or anti-laminin 2α rat IgG monoclonal antibody (4H8-2, Sigma–Aldrich, St. Louis, MO) was used as the initial antibody, and goat anti-mouse IgG2a conjugated with Alexa Fluor 546, goat anti-mouse IgG1 antibody conjugated with Alexa Fluor 488, goat anti-rabbit IgG conjugated with Alexa Fluor 635, or goat anti-rat IgG conjugated with Alexa Fluor 488 was used as a second antibody. The anti-myogenin mouse monoclonal antibody (F5D, BD Pharmingen, San Diego, CA) was used for immunocytochemistry. As a methodological control, the primary antibody was omitted. In the cases of fluorescence, the slides were incubated with Alexa Fluor 546-conjugated goat anti-mouse IgG antibody.

GeneChip expression analysis

Human genome-wide gene expression was examined with the Human Genome U133 Plus 2.0 Array (GeneChip; Affymetrix, Inc., Santa Clara, CA), which contains the oligonucleotide probe set for more than 47,000 transcripts and variants, including approximately 40,000 well-characterized human genes and expressed sequence tags (ESTs). Total RNA was prepared from samples using the RNeasy Kit (Qiagen, Hilden, Germany), according to the manufacturer's instructions. The purity of RNA was assessed on the Agilent Bioanalyser 2100. Double-stranded cDNA was synthesized from DNase-treated total RNA, and the cDNA was subjected to in vitro transcription in the presence of biotinylated nucleoside triphosphates using the Enzo BioArray HighYield RNA Transcript Labeling Kit (Enzo Life Sciences, Inc., Farmingdale, NY) according to the manufacturer's protocol. The biotinylated cRNA was hybridized with a probe array for 16 h at 45°C, and the hybridized biotinylated cRNA was stained with streptavidin–PE (query 6) and scanned with a Hewlett-Packard Gene Array Scanner (Palo Alto, CA). The fluorescence intensity of each probe was quantified using the GeneChip Analysis Suite 5.0 computer program (Affymetrix) and Robust Multi-array Average (RMA) model (Bolstad et al., 2003; Irizarry et al., 2003a,b). To normalize the variations in staining intensity among chips, the "average difference" values for all genes on a given chip were divided by the median value for expression of all genes on the chip. To eliminate genes containing only a background signal, genes were selected only if the raw values of the "average difference" were more than 200, and if the expression of the gene was judged to be "present" by the GeneChip Operating Software version 1.4 (Affymetrix).

Hierarchical clustering and principal component analysis (PCA)

The hierarchical clustering and PCA techniques classify data by similarity of expression pattern using NIA Array Analysis and TIGR Mev (http://lgsun.grc.nia.nih.gov/ANOVA/, http://www.tm4.org/mev.html).

Results

Morphology of placenta-derived cells

We collected 45 normal full-term placentas which were then separated into six parts, that is, UC, AE, AM, CP, VC, and DB (Fig. 1). Ten placentas were used for the subsequent experiments. Primary cells from each separated part were successfully cultured. These cultured cells appeared to be two morphologically different groups: small fibroblast-like cells and epithelium-like cells (Fig. 2Aa–g). Cells derived from the UC, AM, CP, VC, and DB showed fibroblast-like morphology. However, AE-derived cells and some DB-derived cells exhibited a small cobblestone-like morphology. We obtained 1×10^6 cells after 3-week cultivation of 1 cm^3 of UC, AM, CP, and VC; and 1×10^6 cells after 4-week cultivation of 1 cm^3 of AE and DB.

Surface marker expression and gene chip analysis

Surface markers of primary culture placenta-derived cells, in the absence of any inductive stimuli, were evaluated by flow cytometric analysis (Fig. 2B, Supplementary Figs. 1–5). The cells in "early" primary culture (with low replication number) exhibited a heterogeneous pattern by flow cytometric analysis as shown in Supplementary Figure 5. The "CP" shows two peaks (61.1% positive and 38.9% negative) for CD29 (Supplementary Fig. 5A), and the "DB" contains cells negative for CD29 (8.0%) (Supplementary Fig. 5B). In contrast, the cells in "late" primary culture (with high replication number) show a homogenous pattern by flow cytometric analysis due to the culture conditions in which mesenchymal cells can predominantly proliferate. UC-, AE-, AM-, CP-, VC-, and DB-derived cells were positive for CD13, CD29, CD44, CD55, CD59, CD73, CD90, CD105, and CD166. Placenta-derived cells expressed neither hematopoietic lineage markers, such as CD34, nor monocyte-macrophage antigens, such as CD14 (a marker for macrophage and dendritic cells), or CD45 (leukocyte common antigen). The lack of expression of CD14, CD34, or CD45 suggests that all cells cultured in our experimental setting are depleted of hematopoietic cells. The cell population was positive for HLA-ABC, but not for HLA-DR. Among the placenta-derived cells, that is, UC-, AM-, AE-, CP-, VC-, and DB-derived cells, no significant difference was observed in the expression of mesenchymal stem cell markers, suggesting that the cells are of mesenchymal origin or stromal origin.

To clarify the specific gene expression profile of cells derived from each portion of the placenta, we compared the expression levels using Affymetrix GeneChip oligonucleotide arrays. RNAs were isolated from primary cultured cells of the placenta. The gene expression profile reported in this article has been deposited in the gene Expression Omnibus (GEO) database (http://www.ncbi.nlm.gov/geo: accession no. GSM289889-289894). We performed PCA to determine whether it is possible to discriminate cells of one part from cells of other parts in two-dimensional expression space. PCA, using all probes and 1,087 probes which were annotated with the "transcription factor," revealed that the DB-derived cells are categorized into a distinct group. Statistical analysis revealed that the DB-derived cells significantly express genes for *FOXL2, HOP, HOXD10, HOXD11*, and *HOXA5*. We thus analyzed the *HOX* genes by hierarchical clustering and PCA, since the cells are well categorized, especially based on the *HOX* gene family, and identified three clusters (Fig. 2C,D). Determination of cell specification via gene chip analysis revealed that the each placental cell has a distinct expression pattern of the *HOX* gene family: (a) AE- and AM-derived cells preferentially express the *HOX B* genes, such as *HOX B2, B6, B7*, and *B8*; (b) DB-derived cells express the *HOX D* genes, such as *D3, D4, D8, D9, D10*, and *D11*; (c) the others express the *HOX A* genes, *HOXA13* and *A3*.

In vitro induction of myogenic differentiation

Each distinct part of the placenta has recently been viewed as a candidate source of material for cell-based therapies. We examined, both in vitro and in vivo, whether the placenta-derived cells have a myogenic potential. Of the 54,675 genes represented on the GeneChip, skeletal muscle-specific genes such as the phospholamban, myozenin, dystrobrevin, and myosin heavy chain were expressed in cells derived from VC and the CP. Expression of these muscle-specific genes in these cells led us to hypothesize that these cells are capable of differentiating into myocytes. To prove this, cells from each part of the placenta were exposed to 5-azacytidine for 24 h and then

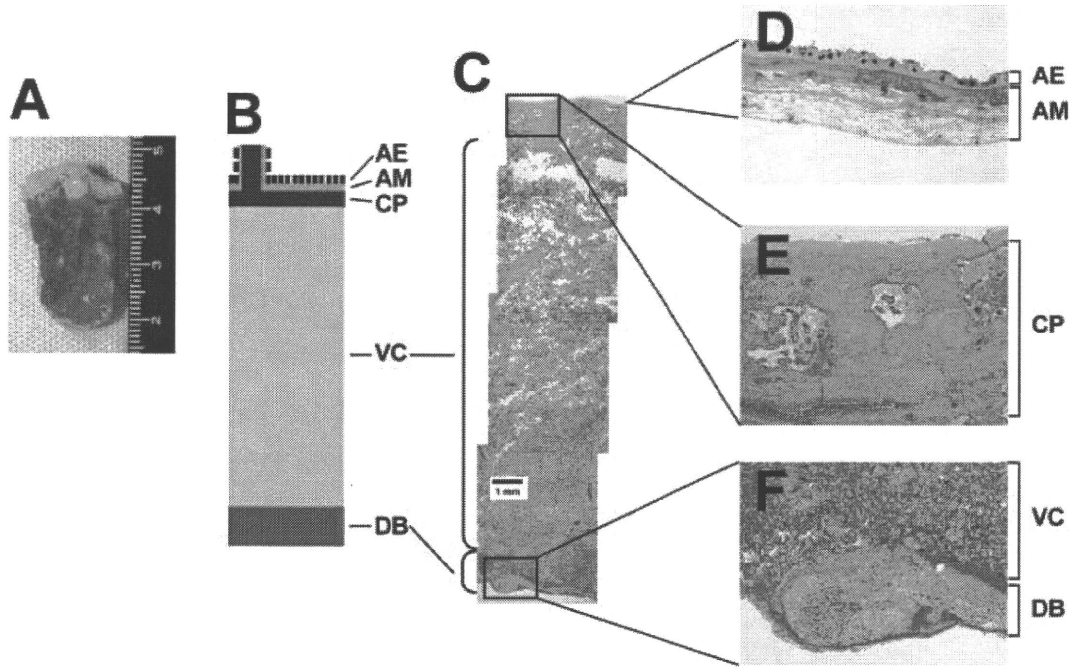

Fig. 1. Placenta-derived cells from each portion. Macroscopy (A) and histology (B,C) of amnion (D), chorionic plate (E), villous chorion, and decidua basalis (F). AE, amniotic epithelium; AM, amniotic mesoderm; CP, chorionic plate; VC, villous chorion; DB, decidua basalis.

cultured in DMEM supplemented with 2% horse serum for 3 weeks. Myogenic differentiation of the cells was analyzed by evaluating the expression of MyoD, Myf5, myogenin, MyHC-IIx/d, and desmin by RT-PCR and immunocytochemistry (Fig. 3). MyoD is constitutively expressed in amniotic mesodermal cells but decreased to no measurable level at day 3 and thereafter (Fig. 3A). In the case of the CP and VC, MyoD expression is detected at 3 weeks. Expression of genes encoding MyoD, Myf5, myogenin, and MyHC-IIx/d was under a detectable level in cells derived from UC, AE, and DB even after myogenic induction. MyHC-IIx/d, a structural gene, started to be expressed at the middle of differentiation in amniotic mesodermal cells and at the late stage in CP-derived cells. Desmin was expressed in cells derived from AM, UC, CP, AE, and DB throughout differentiation. In the cells derived from AM and CP, dystrophin expression increased after myogenic induction (Fig. 3B). Immunocytochemical analysis revealed that CP-derived cells became positive for MyHC-IIx/d, α-sarcoglycan, and myogenin after cultivation with 2% horse serum for 21 days (Fig. 3C–E). However, without any treatment, the cells did not show myotube-like morphology (Fig. 3Cc). C2C12 myoblasts were used for a positive control of immunocytochemistry (Supplementary Fig. 6). Placenta-derived cells from each portion exhibit different capabilities for proliferation and myogenesis in vitro (Fig. 3F).

Detection of human placental cell contribution to myotubes in an in vitro myogenesis model

To simulate in vivo phenomena, human placental cells were co-cultured in vitro with murine C2C12 myoblasts for 2 days under proliferative conditions and then switched to differentiation conditions for an additional 7 days. Multinucleated myotubes were formed after co-culturing with C2C12 cells (Fig. 4). Myosin heavy chain and human nuclei were unequivocally identified by staining with MF20 and an antibody to human nuclei, while the numerous mouse nuclei present in this field, as shown by DAPI staining, are negative. The frequency of fusion between placenta-derived cells and C2C12 myotube depends on the cell type: cells derived from CP and DB exhibited high frequencies of fusion, whereas cells derived from AE and UC induced low-level fusion to C2C12 myocytes. No multinucleated cells were formed without co-cultivation.

Expression of human dystrophin by cell implantation in the mdx-scid mouse

To investigate whether placenta-derived cells can generate muscle tissue in vivo, cells (2×10^7) without any treatment or induction were implanted directly into the right anterior tibialis muscles of mdx-scid mice. PBS without cells was injected into the left anterior tibialis muscle as a control. After 4 weeks, myofibers in the muscle tissues injected with amniotic mesodermal cells expressed human dystrophin and laminin (Fig. 5). Dystrophin was not detected in the muscle of mdx-scid mice without cell implantation because the antibody to dystrophin used in this study is human-specific, implying that dystrophin is transcribed from dystrophin genes of human donor cells but not from reversion of dystrophied myocytes in mdx-scid mice.

Discussion

Differential myogenic potential of cultured cells from each part of the placenta

The placenta includes cells of maternal and fetal origin. Although most placenta-derived cells are of extraembryonic origin, AE-derived cells are from the epiblast/inner cell mass of the blastocyst (Cunningham and Williams, 2005; Sadler and Langman, 2006). The aim of this study was to determine the intrinsic differentiation potential of cells from six parts of the

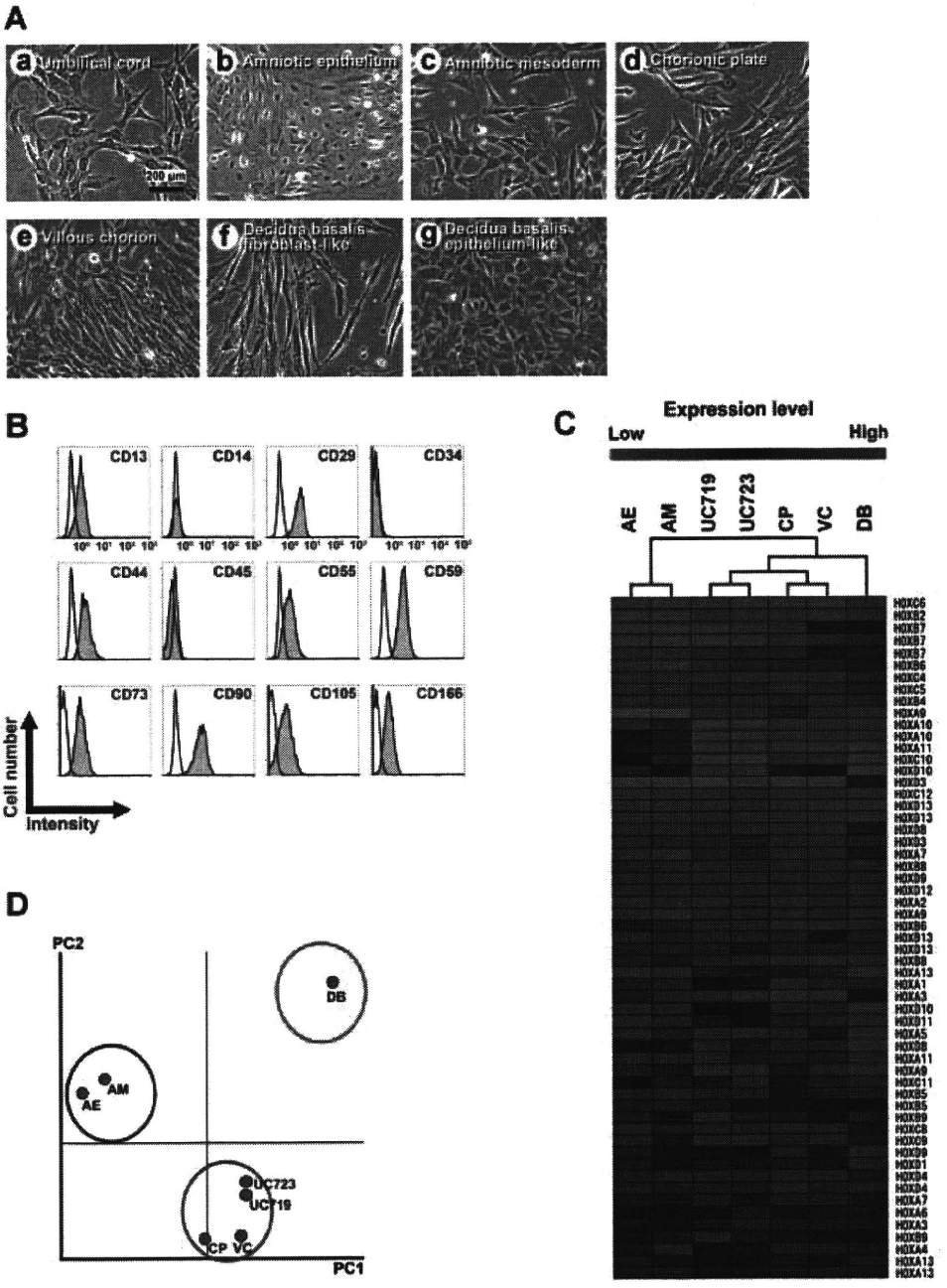

Fig. 2. Morphology of placenta-derived cells and flow cytometric analysis of amniotic mesoderm-derived cells. A: Photomicrographs of cells from umbilical cord-derived cells (a), amniotic epithelial cells (b), amniotic mesodermal cells (c), chorionic plate-derived cells (d), villous chorion-derived cells (e), decidua basalis-derived cells (f: fibroblast-like, g: epithelial cell-like) from primary culture. Amniotic epithelial cells (b) and decidua basalis-derived cells (g) showed an epithelial cell-like (cobblestone-like) morphology, while the others (a,c,d,e,f) showed a fibroblast-like morphology. Scale bars: 200 μm. B: Flow cytometric analysis of amniotic mesoderm-derived cells in primary culture (with high replication number) in the absence of any inductive stimuli. Non-shaded and shaded areas indicated reactivity of antibodies for isotype controls and that of antibodies for cell surface markers, respectively. C: Hierarchical clustering analysis and heat map analysis of *HOX* gene expression in cells derived from umbilical cord (UC719 and UC723), amniotic epithelium (AE), amniotic mesoderm, (AM), chorionic plate (CP), villous chorion (VC), decidua basalis (DB), using "TIGR MeV." D: PCA revealing general trends of *HOX* gene expression.

placenta, that is, UC, AE, AM, CP, VC, and DB. The myogenic potential of cells from the AM, CP, and VC proved much greater than expected, and this higher myogenic differentiation ratio can be a reflection of the intrinsic cellular potential of extraembryonic mesodermal cells. Lack of myogenic potential in AE-derived cells is envisaged because the cells are of extraembryonic ectodermal origin and cuboidal in morphology.

Despite our findings, amniotic epithelial cells have been reported to have the potential to differentiate to all three germ layer cells, including myocytes, after in vitro sphere formation (Miki et al., 2005). Amniotic epithelial cells formed neither spheres nor viable supernatant cells in our experimental settings, but displayed a cobblestone appearance with an epithelial phenotype. Cells obtained from AE, we believe,

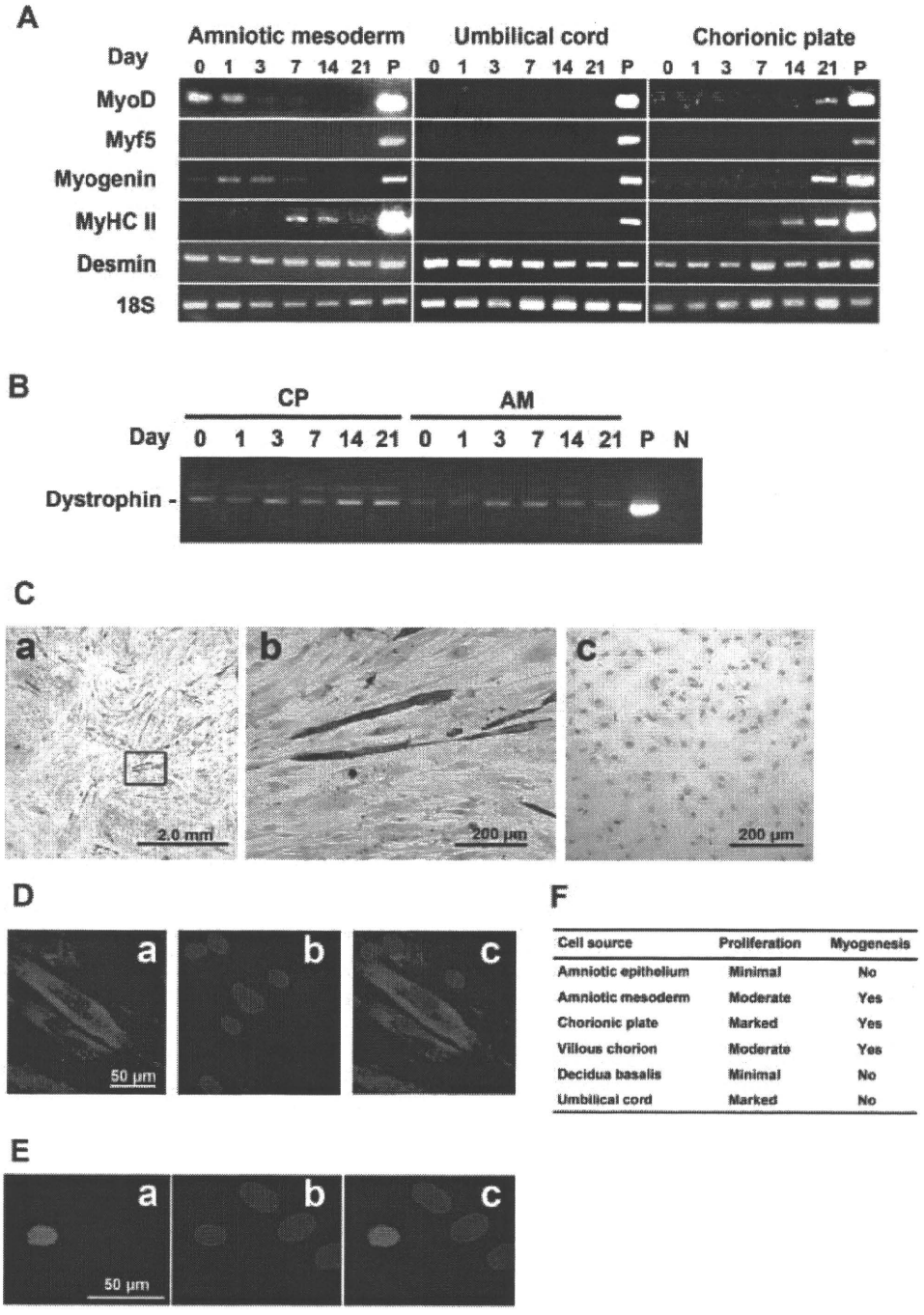

Cell source	Proliferation	Myogenesis
Amniotic epithelium	Minimal	No
Amniotic mesoderm	Moderate	Yes
Chorionic plate	Marked	Yes
Villous chorion	Moderate	Yes
Decidua basalis	Minimal	No
Umbilical cord	Marked	No

Fig. 3. Expression of muscle-specific genes during differentiation of placenta-derived cells. A: RT-PCR analysis of human MyoD, Myf5, myogenin, myosin heavy chain type IIx/d (MyHC-IIx/d), desmin, and 18S cDNA (from top to bottom). Amniotic mesodermal cells, umbilical cord-derived cells, and chorionic plate-derived cells were exposed to 5 μM 5-azacytidine for 24 h and then subsequently cultured in DMEM supplemented with 2% HS for 21 days. RNAs from human muscle serve as a positive (P) control. Only the 18S PCR primer used as a positive control reacted with the human and murine cDNA. B: RT-PCR analysis of human dystrophin in chorionic plate (CP) and amniotic mesodermal cells (AM). The muscle-specific isoform (Dp427m) was amplified. RNAs from human muscle serve as a positive (P) control. C: Immunocytochemistry of skeletal myosin heavy chain in chorionic plate-derived cells after myogenic induction (a,b) or no induction (c). Scale bars: (a) 2.0 mm, (b,c) 200 μm. D: Immunocytochemistry of α-sarcoglycan. a: α-sarcoglycan; b: DAPI staining; c: "merge" of a and b. Scale bars: 50 μm. E: Immunocytochemistry of myogenin. a: myogenin; b: DAPI staining; c: "merge" of a and b. Scale bars: 50 μm. F: Cell site origin and capability for proliferation and myogenesis.

correspond to previously reported adherent cells with little myogenic activity (Miki et al., 2005). The poor myogenic capability of UC-derived cells was also contrary to our expectation based on prior research (Conconi et al., 2006). It may also be due to intrinsic cell characteristics (or cell mission), and UC-derived cells embedded in Wharton's jelly may be terminally differentiated cells or highly specific cells which produce a matrix for cushioning of the cord.

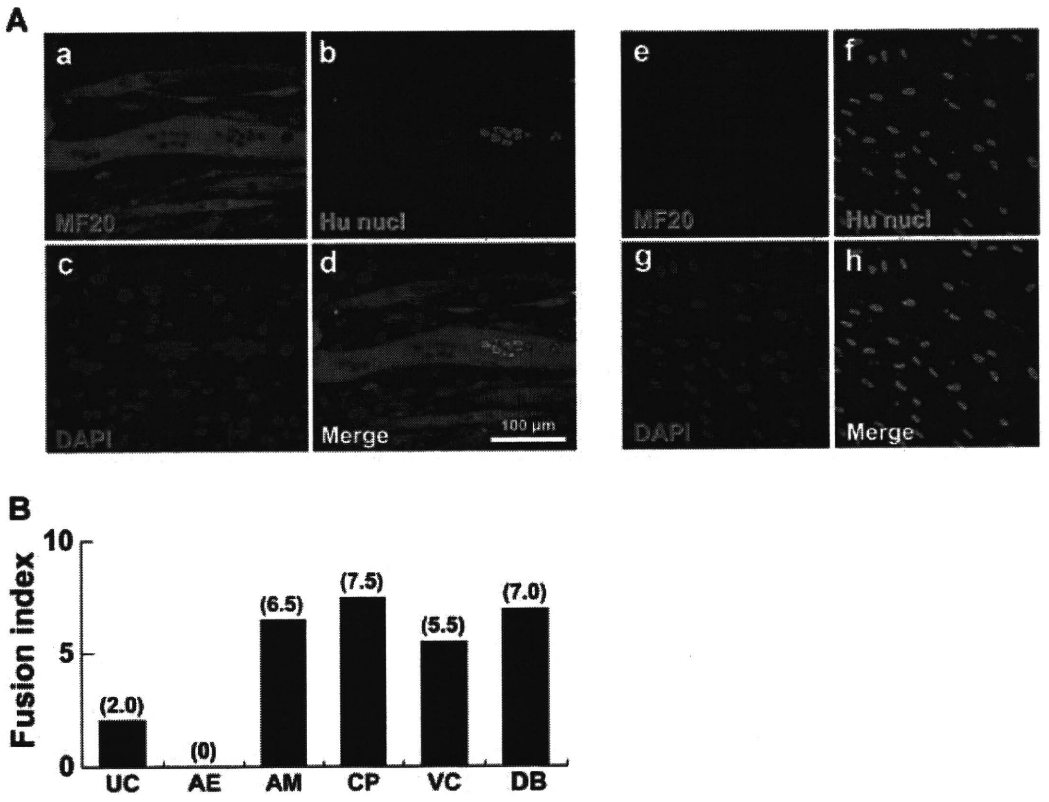

Fig. 4. Detection of human placenta-derived cell contribution to myotubes in an in vitro myogenesis model. The chorionic plate-derived cells were co-cultured with C2C12 myoblasts for 2 days under conditions that favored proliferation. The cultures were then changed to differentiation media for 7 days to induce myogenic fusion. A: Fusion between human chorionic plate-derived cells and murine C2C12 cells. a: human myosin heavy chain molecule (red, MF20); b: human nuclei (HuNucl, green); c: DAPI staining (blue); d: "merge" of a, b, and c. Scale bars: 100 μm. e–h: Human chorionic plate-derived cells without co-culturing. e: human myosin heavy chain molecule (red, MF20); f: human nuclei (HuNucl, green); g: DAPI staining (blue); h: "merge" of e, f, and g. B: Comparison of fusion between each placenta-derived cell and mouse C2C12 myoblasts. Fusion index is shown as number of fused cells per 1,000 cells. UC, umbilical cord; AE, amniotic epithelium; AM, amniotic mesoderm; CP, chorionic plate; VC, villous chorion; DB, decidua basalis.

Taxonomic approach using global gene expression database

In general, cultured cells reflect in vivo characteristics, for example, hematopoietic cells proliferate as a supernatant cell in culture, and epithelial cells exhibit cobblestone appearance at confluence. In contrast, mesenchymal/stromal cells from each part of the placenta, regardless of cell source, show similar appearance in vitro and in vivo, irrespective of their diversity with respect to differentiation and proliferation. The different phenotypes of mesenchymal/stromal cells are maintained even after a series of cell replications and passages, probably by epigenetics, such as genomic methylation and chromatin of cells. The stably transmitted epigenetics in cultured cells reflects a gene expression network and maintains cell identity, and thus each mesenchymal cell is predictable by the results of gene expression with GeneChip analysis. Categorization of the cells may reflect the native functional difference, even after cultivation, and implies that cells from the UC, AE, AM, CP, VC, and DB have a distinct cell identity, in addition to mesenchymal or epithelial phenotypes.

Cell-based therapy for DMD

DMD is a fatal disease for which an effective treatment is still being actively sought. As a novel treatment option, stem cells could be used to replace defective dystrophin and restore the dystrophic muscles. Most placenta-derived cells are either myogenic progenitors or have myogenic potential, and clearly cells with the highest myogenic potential would be beneficial for treatment of dystrophic muscle. Acquisition or recovery of dystrophin expression in dystrophic muscle is attributed to two different mechanisms: (a) myogenic differentiation of implanted or transplanted cells and (b) cell fusion of implanted or transplanted cells with host muscle cells. In this study using placenta-derived cells, our findings, namely that implantation of placenta-derived cells improved the efficiency of muscle regeneration and dystrophin delivery to dystrophic muscle in mice, are explained by both possibilities or the latter possibility (fusion mechanism) alone. Efficient fusion systems of placenta-derived cells with host dystrophic myocytes may contribute substantially to a major advance toward eventual cell-based therapies for muscle injury or chronic muscular disease.

The isolation of tissue-specific stem cells for expansion in vitro and transplantation back into the patient in an allogeneic manner is indeed an ideal strategy, from the viewpoint of industry-based, sustainable supply of large quantities of affordable, quality-controlled cells. In most cases of degenerative diseases and genetic diseases, such as lysosomal storage diseases, it is unlikely that enough unaffected stem cells will be isolated or available in sufficient quantity, necessitating the use of stem cells from suitable, cost-effective allogeneic sources, such as human placenta. The predicted number of AM-derived cells from one placenta of an average size (500 g)

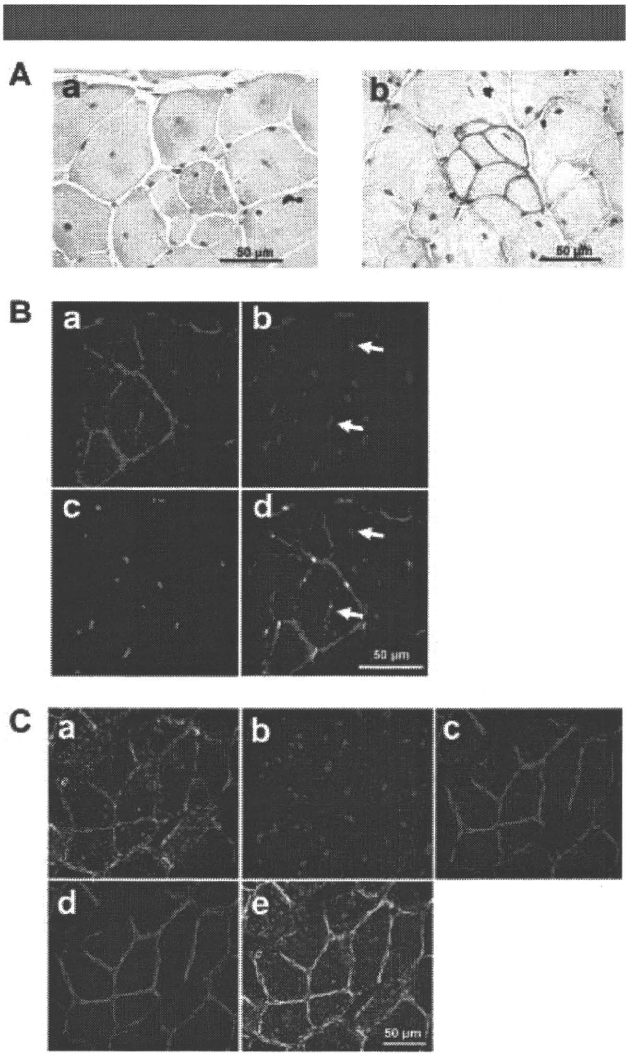

Fig. 5. Conferral of dystrophin to mdx myocytes by human placenta-derived cells. A: Immunohistochemistry using an antibody against human dystrophin on anterior tibialis muscle sections of mdx-scid mice after direct injection of PBS without cells (a: negative control) or amniotic mesoderm-derived cells without any treatment or induction (b) into mdx-scid myofibers. Scale bars: 50 μm. B: Immunohistochemistry analysis on anterior tibialis muscle sections of mdx-scid mice after direct injection of amniotic mesoderm-derived cells without any treatment or induction. Immunohistochemistry revealed the incorporation of implanted cells into newly formed myofibers, which expressed human dystrophin 4 weeks after implantation. Murine nuclei are indicated by arrows. a: human dystrophin molecule (red); b: DAPI staining (blue); c: human nuclei (HuNucl, green); d: "merge" of a, b, and c. Scale bars: 50 μm. C: Immunohistochemistry analysis on anterior tibialis muscle sections of mdx-scid mice after direct injection of amniotic mesoderm-derived cells. a: α-sarcoglycan (yellow); b: DAPI staining (blue); c: laminin (red); d: human dystrophin (green); e: "merge" of a, b, c, and d. Scale bars: 50 μm.

would be approximately 1×10^6 (before ex vivo amplification), possibly reaching 1×10^{11} after cultivation. This may cover 3,000 cm^3 of muscular tissues in cell-based therapy (Skuk et al., 2006). Cells converted into myotubes in vitro at a high frequency after induction, giving rise to large numbers of myofibers expressing human dystrophin when transplanted into BALB/c and mdx mice, thus fulfilling all the criteria required for a successful allogeneic cell therapy for muscular dystrophy. It should also be remembered that currently, implantation of placenta-derived cells in an allogeneic combination requires administration of immunosuppressive drugs, such as FK506 and steroids.

We have established a method for systemic mapping of placental cells with myogenic potential. Cellular dissection and cultivation, coupled with accurate determination of the molecular characteristics of specific cells in the human placenta, opens up significant new possibilities in regenerative medicine. The outcome of this study indicates a potential cell-based treatment for DMD, a lethal human disease for which no effective treatment currently exists.

Acknowledgments

We would like to express our sincere thanks to H. Abe and M. Inoue-Yamazaki for providing expert technical assistance, to K. Saito for her secretarial work, and to A. Crump for reviewing the manuscript.

Literature Cited

Barton-Davis ER, Cordier L, Shoturma DI, Leland SE, Sweeney HL. 1999. Aminoglycoside antibiotics restore dystrophin function to skeletal muscles of mdx mice. J Clin Invest 104:375–381.

Bolstad BM, Irizarry RA, Astrand M, Speed TP. 2003. A comparison of normalization methods for high density oligonucleotide array data based on variance and bias. Bioinformatics 19:185–193.

Conconi MT, Burra P, Di Liddo R, Calore C, Turetta M, Bellini S, Bo P, Nussdorfer GG, Parnigotto PP. 2006. CD105(+) cells from Wharton's jelly show in vitro and in vivo myogenic differentiative potential. Int J Mol Med 18:1089–1096.

Cossu G, Mavilio F. 2000. Myogenic stem cells for the therapy of primary myopathies: Wishful thinking or therapeutic perspective? J Clin Invest 105:1669–1674.

Cui CH, Uyama T, Miyado K, Terai M, Kyo S, Kiyono T, Umezawa A. 2007. Menstrual blood-derived cells confer human dystrophin expression in the murine model of Duchenne muscular dystrophy via cell fusion and myogenic transdifferentiation. Mol Biol Cell 18:1586–1594.

Cunningham FG, Williams JW. 2005. Implantation, embryogenesis, and placenta development. In: Williams obstetrics, 22nd edition. New York: McGraw-Hill Professional. pp 39–90.

Dezawa M, Ishikawa H, Itokazu Y, Yoshihara T, Hoshino M, Takeda S, Ide C, Nabeshima Y. 2005. Bone marrow stromal cells generate muscle cells and repair muscle degeneration. Science 309:314–317.

Di Rocco G, Iachininoto MG, Tritarelli A, Straino S, Zacheo A, Germani A, Crea F, Capogrossi MC. 2006. Myogenic potential of adipose-tissue-derived cells. J Cell Sci 119:2945–2952.

Ervasti JM, Campbell KP. 1991. Membrane organization of the dystrophin-glycoprotein complex. Cell 66:1121–1131.

Ferrari G, Cusella-De Angelis G, Coletta M, Paolucci E, Stornaiuolo A, Cossu G, Mavilio F. 1998. Muscle regeneration by bone marrow-derived myogenic progenitors. Science 279:1528–1530.

Fukuchi Y, Nakajima H, Sugiyama D, Hirose I, Kitamura T, Tsuji K. 2004. Human placenta-derived cells have mesenchymal stem/progenitor cell potential. Stem Cells 22:649–658.

Gang EJ, Jeong JA, Hong SH, Hwang SH, Kim SW, Yang IH, Ahn C, Han H, Kim H. 2004. Skeletal myogenic differentiation of mesenchymal stem cells isolated from human umbilical cord blood. Stem Cells 22:617–624.

Grounds MD, White JD, Rosenthal N, Bogoyevitch MA. 2002. The role of stem cells in skeletal and cardiac muscle repair. J Histochem Cytochem 50:589–610.

Harper SQ, Hauser MA, DelloRusso C, Duan D, Crawford RW, Phelps SF, Harper HA, Robinson AS, Engelhardt JF, Brooks SV, Chamberlain JS. 2002. Modular flexibility of dystrophin: Implications for gene therapy of Duchenne muscular dystrophy. Nat Med 8:253–261.

Irizarry RA, Bolstad BM, Collin F, Cope LM, Hobbs B, Speed TP. 2003a. Summaries of Affymetrix GeneChip probe level data. Nucleic Acids Res 31:e15.

Irizarry RA, Hobbs B, Collin F, Beazer-Barclay YD, Antonellis KJ, Scherf U, Speed TP. 2003b. Exploration, normalization, and summaries of high density oligonucleotide array probe level data. Biostatistics 4:249–264.

Matsuo M, Masumura T, Nishio H, Nakajima T, Kitoh Y, Takumi T, Koga J, Nakamura H. 1991. Exon skipping during splicing of dystrophin mRNA precursor due to an intraexon deletion in the dystrophin gene of Duchenne muscular dystrophy kobe. J Clin Invest 87:2127–2131.

Miki T, Lehmann T, Cai H, Stolz DB, Strom SC. 2005. Stem cell characteristics of amniotic epithelial cells. Stem Cells 23:1549–1559.

Mori T, Kiyono T, Imabayashi H, Takeda Y, Tsuchiya K, Miyoshi S, Makino H, Matsumoto K, Saito H, Ogawa S, Sakamoto M, Hata J, Umezawa A. 2005. Combination of hTERT and bmi-1, E6, or E7 induces prolongation of the life span of bone marrow stromal cells from an elderly donor without affecting their neurogenic potential. Mol Cell Biol 25:5183–5195.

Portmann-Lanz CB, Schoeberlein A, Huber A, Sager R, Malek A, Holzgreve W, Surbek DV. 2006. Placental mesenchymal stem cells as potential autologous graft for pre- and perinatal neuroregeneration. Am J Obstet Gynecol 194:664–673.

Rodriguez AM, Pisani D, Dechesne CA, Turc-Carel C, Kurzenne JY, Wdziekonski B, Villageois A, Bagnis C, Breittmayer JP, Groux H, Ailhaud G, Dani C. 2005. Transplantation of a multipotent cell population from human adipose tissue induces dystrophin expression in the immunocompetent mdx mouse. J Exp Med 201:1397–1405.

Sadler TW, Langman J. 2006. Third month to birth: The fetus and placenta. In: Langman's medical embryology, 10th edition. Philadelphia: Lippincott Williams & Wilkins. pp 89–109.

Skuk D, Goulet M, Roy B, Chapdelaine P, Bouchard JP, Roy R, Dugre FJ, Sylvain M, Lachance JG, Deschenes L, Senay H, Tremblay JP. 2006. Dystrophin expression in muscles of duchenne muscular dystrophy patients after high-density injections of normal myogenic cells. J Neuropathol Exp Neurol 65:371–386.

Terai M, Uyama T, Sugiki T, Li XK, Umezawa A, Kiyono T. 2005. Immortalization of human fetal cells: The life span of umbilical cord blood-derived cells can be prolonged without manipulating p16INK4a/RB braking pathway. Mol Biol Cell 16:1491–1499.

脊髄性筋萎縮症

斎藤加代子　伊藤万由里　荒川玲子　東京女子医科大学附属遺伝子医療センター

はじめに

脊髄性筋萎縮症(SMA)は脊髄の前角細胞の変性による筋萎縮と進行性筋力低下を特徴とする常染色体劣性遺伝病である．SMAの遺伝子同定のためには明確な診断基準と分類を確立することが必要であるという考えのもとに，国際SMA協会が組織され，**図1**に示す診断基準が作成された[1]．さらに2009年にはわが国の厚生労働科学研究費補助金(難治性疾患克服研究事業)神経変性疾患に関する調査研究班において**図2**のような診断基準が作成された[2]．

従来，広義の脊髄性進行性筋萎縮症(SPMA)として，小児期発症のSMAと成人発症のSPMAを総称してSPMAとしており，わが国の難治性疾患克服研究事業において，SPMAの疾患名が使用されていた．海外の成書や論文では，「広義のSPMA」という表現は使用されておらず，「広義のSMA」として表わされている．さらに，ICD-10では，「G-12：脊髄性筋萎縮症及び関連症候群」のなかに，G-122：脊髄性進行性筋萎縮症，G-129脊髄性筋萎縮症が含まれている．そこで2009年に国際的な表現に統一を図るため，「脊髄性筋萎縮症(SMA)」となった．

小児期特に乳幼児期発症のSMAの多くはsurvivial motor neuron (SMN)遺伝子に変異を示すSMAであり，成人発症例や図1の除外項目に当てはまるような所見を示す場合，遺伝子的に異質である可能性が高い．本稿では遺伝子診断が可能であるSMAとして，SMN遺伝子に変異を示すSMAを中心として述べる．

■図1　脊髄性筋萎縮症の診断基準

包含項目	除外項目
Ⅰ．筋力低下 対称性 近位筋＞遠位筋 下肢＞上肢 躯幹および四肢	1．中枢神経機能障害 2．関節拘縮症 3．外眼筋，横隔膜，心筋の障害，聴覚障害，著しい顔面筋罹患
Ⅱ．脱神経 舌の線維束性収縮 手の振戦	4．知覚障害 5．血清CK値＞正常上限の10倍
筋生検―萎縮筋線維の群 筋電図―神経原性変化	6．運動神経伝導速度＜正常下限の70% 7．知覚神経活動電位の異常

(国際SMA協会報告，1992)

■図2　脊髄性筋萎縮症の特定疾患診断基準

1．主要項目
(1)臨床所見
①下記のような下位運動ニューロン症候を認める．
筋力低下
筋萎縮
舌，手指の線維束性収縮 fasciculation
腱反射は減弱から消失
②下記のような上位運動ニューロン症候は認めない．
痙縮
腱反射亢進
病的反射陽性
③経過は進行性である．
(2)臨床検査所見
筋電図で高振幅電位や多相性電位等の神経原性所見を認める．
(3)遺伝子診断
survival motor neuron (SMN) 遺伝子変異を認める．
2．鑑別診断
(1)　筋萎縮性側索硬化症
(2)　球脊髄性筋萎縮症
(3)　脳腫瘍・脊髄疾患
(4)　頸椎症，椎間板ヘルニア，脳および脊髄腫瘍，脊髄空洞症等
(5)　末梢神経疾患
(6)　多発性神経炎(遺伝性，非遺伝性)，多発限局性運動性末梢神経炎 multifocal motor neuropathy 等
(7)　筋疾患：筋ジストロフィー，多発筋炎等
(8)　感染症に関連した下位運動ニューロン障害：ポリオ後症候群等
(9)　傍腫瘍症候群
(10)　先天性多発性関節拘縮症
(11)　神経筋接合部疾患
3．診断の判定
上記1の(1)①②③すべてと(2)，(3)の1項目以上を満たし，かつ2のいずれでもない．

(厚生労働省神経変性疾患調査研究班(中野今治班長)，2009)

■図5　Multiplex Ligation-dependent Probe Amplification (MLPA)法によるSMAの遺伝子診断

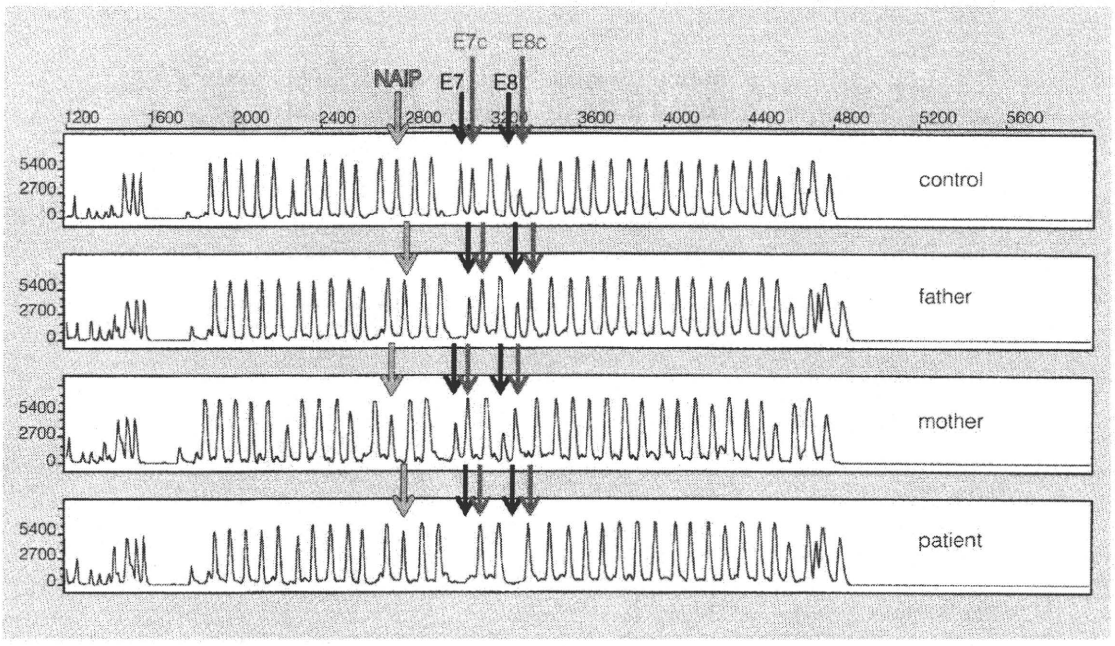

■図6　SMAの型による症状の差の説明

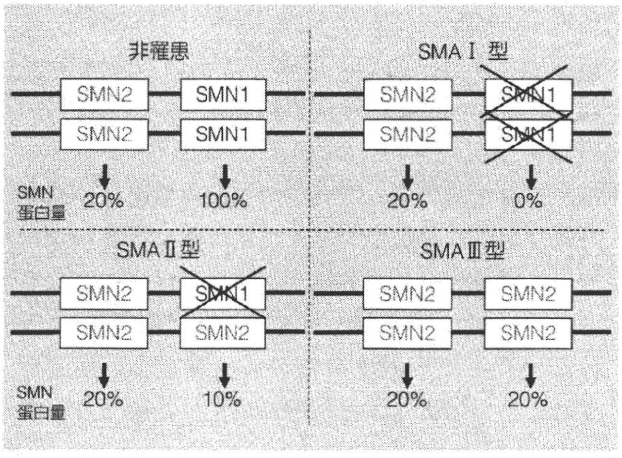

(Wirth et al, 2006)[11]

遺伝子欠失ではなく遺伝子変換によりSMN1遺伝子がSMN2遺伝子になること，すなわちSMN2遺伝子の遺伝子産物の量が多くなっている．正常ではSMN蛋白量が120%であるとすると，SMA Ⅰ型は20%，Ⅱ型は30%，Ⅲ型は40%と考えられ，臨床症状の重症から軽症の幅の説明となっている[11]．

SMAに似ているが，典型的SMAとは異なった病因，病態の疾患が存在する．染色体5qのマーカーに連鎖しておらず，またSMN遺伝子の欠失も示さず，SMAプラスバリアントというカテゴリーに入る例が存在している[12]．これらには，SMA＋横隔膜麻痺，SMA＋オリーブ橋小脳低形成，SMA＋先天性関節拘縮等があり，これらの遺伝子は染色体5q13にはない．また，常染色体優性遺伝形式のSMAの報告もあるが，この遺伝子も第5染色体にはない．このうち，SMA＋横隔膜麻痺の遺伝子は染色体11q13.2-q13.4に存在する免疫グロブリン・結合蛋白2(IGHMBP2)，SMA＋先天性関節拘縮は染色体5q35のマーカーとの連鎖が報告されている．さらにⅣ型については，複数の病因が考えられる．そのひとつとして，上肢の遠位筋優位なDuchenne-Aran型，distal SMA，progressive muscular atrophyとされる症例の存在があり，Vesicle-associated membrane protein-associated protein B/Cが原因遺伝子のALSであるFinkel type SMA (ALS8)との異同が興味深い．

治療と医療管理

SMAに対する根本的な治療は，いまだ確立していない．しかし，効果が期待できる治療法の研究開発は，主に海外で盛んに行われている．SMN2遺伝子のexon 7のスプライシングパター

■ 図 3　SMA の原因遺伝子 SMN 遺伝子

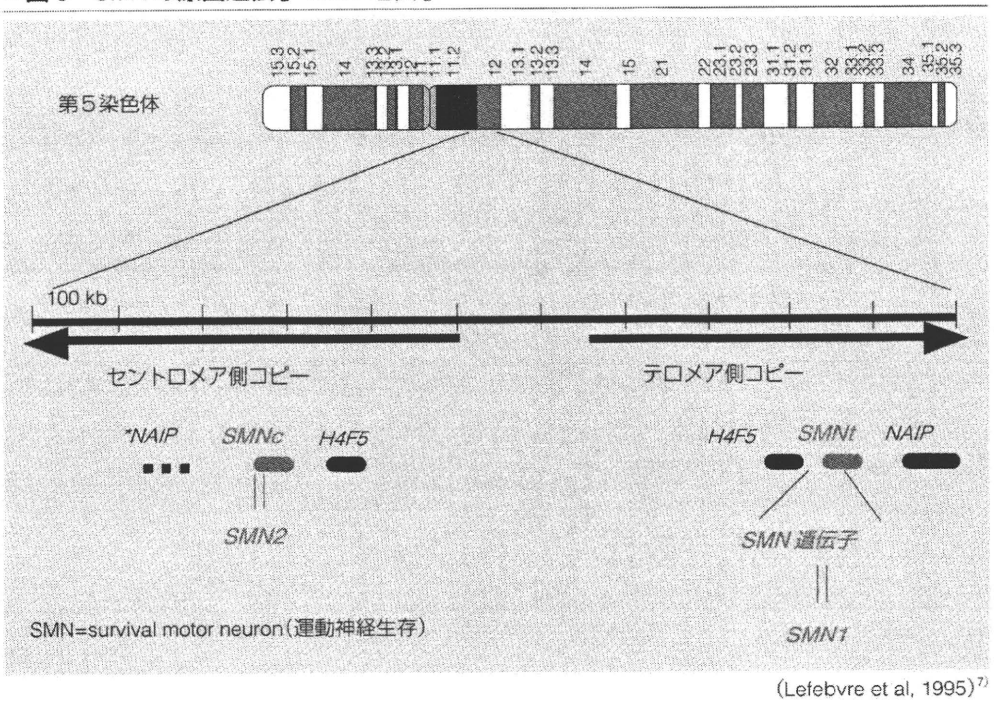

(Lefebvre et al, 1995)[7]

■ 図 4　SMA における SMN 遺伝子欠失と NAIP 遺伝子欠失（自験例）

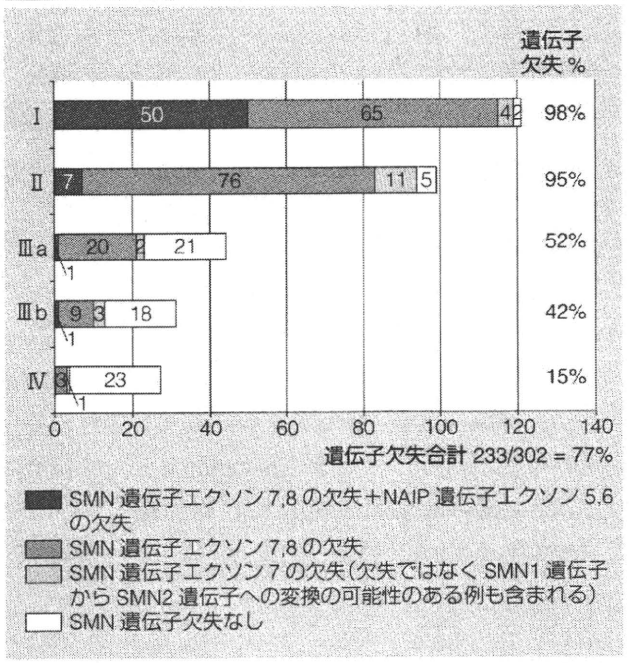

SMA Ⅰ型，Ⅱ型，Ⅲa 型，Ⅲb 型，Ⅳ型における SMN 遺伝子欠失と NAIP 遺伝子欠失を示す割合（横軸は例数，図のなかの数字は各型における実数）

ている SMA のⅡ型とⅢ型において，SMN1 遺伝子のエクソン 7 の 1 塩基が SMN2 遺伝子のエクソン 7 の配列と同様に変換されていたことが明らかになった[10]．したがって，SMN1 遺伝子のエクソン 7 は欠失していたのではなく遺伝子変換されており，重症なⅠ型ではホモ接合性に SMN1 遺伝子のエクソン 7 とエクソン 8 の欠失を有しているが，軽症のⅡ型，Ⅲ型では SMN1 遺伝子のエクソン 7 が SMN2 遺伝子のエクソン 7 に変換されることによって症状が軽症である例も存在する．

最近は，**図 5** のように Multiplex Ligation-dependent Probe Amplification（MLPA）法によって，遺伝子量も明らかにできるようになり，保因者診断も可能となってきている．

SMA の臨床的多様性と遺伝子的多様性

SMA のⅠ型からⅣ型の臨床像の幅については，**図 6** のように SMN 蛋白質の発現量，すなわち SMN2 遺伝子がどの程度，SMN 蛋白質を産生するかで説明できる．臨床像が軽症の場合，SMN